Short Bunch Instabilities

John Byrd

Overview

- Single Pass instabilities
  - CSR microbunching
  - Longitudinal Space Charge
- Impedance sources
- LCLS
  - microbunching gain
  - An effective laser heater to suppress microbunching
- SDL
  - Observations and analysis
- Storage Ring Microbunching instability

Some references

- CSR microbunching
  - Borland *et al*., NIMA (2002) LCLS *elegant* studies
  - Saldin, Schneidmiller, Yurkov, NIMA (2002) Klystron amplification
  - Heifets, Stupakov, Krinsky, PRST-AB (2002) Integral equation
  - Huang, Kim, PRST-AB (2002) Integral equation with iterative solution

- LSC instability
  - Saldin, Schneidmiller, Yurkov, TESLA-FEL-2003-02

- Study of effective Landau damping
  - Huang, Borland, Emma, Wu, Limborg, Stupakov, Welch,
  - SLAC-PUB-10334, 2004

- SDL modulation experiments
  - Graves et al., PAC2001, observations of “microbunching”
  - Shaftan and Huang, BNL-71491 (2003), data analysis and modeling

Single pass instabilities

- high FEL gain (i.e. instability) in the undulator requires very bright electron beams (small emittance and energy spread)

- Such a bright beam interacting with self-fields in the accelerator before the undulator can be sensitive to other “undesirable” instabilities.

- Bunch compressors designed to increase the peak current give rise to a microbunching instability that may degrade the beam quality significantly

- Increasing the local energy spread within the FEL tolerance (**controlled heating**) can damp the undersired instability while keeping an acceptable FEL gain.

How cold is the photoinjector beam?

Parmela at 1 nC

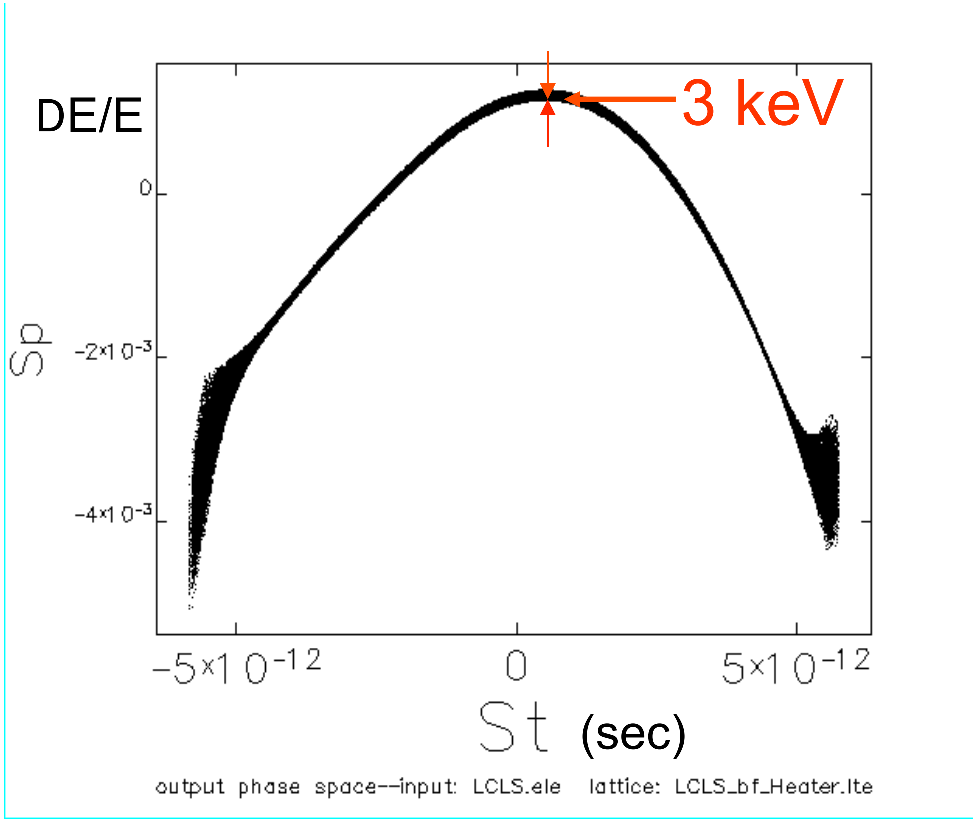

TTF measurement

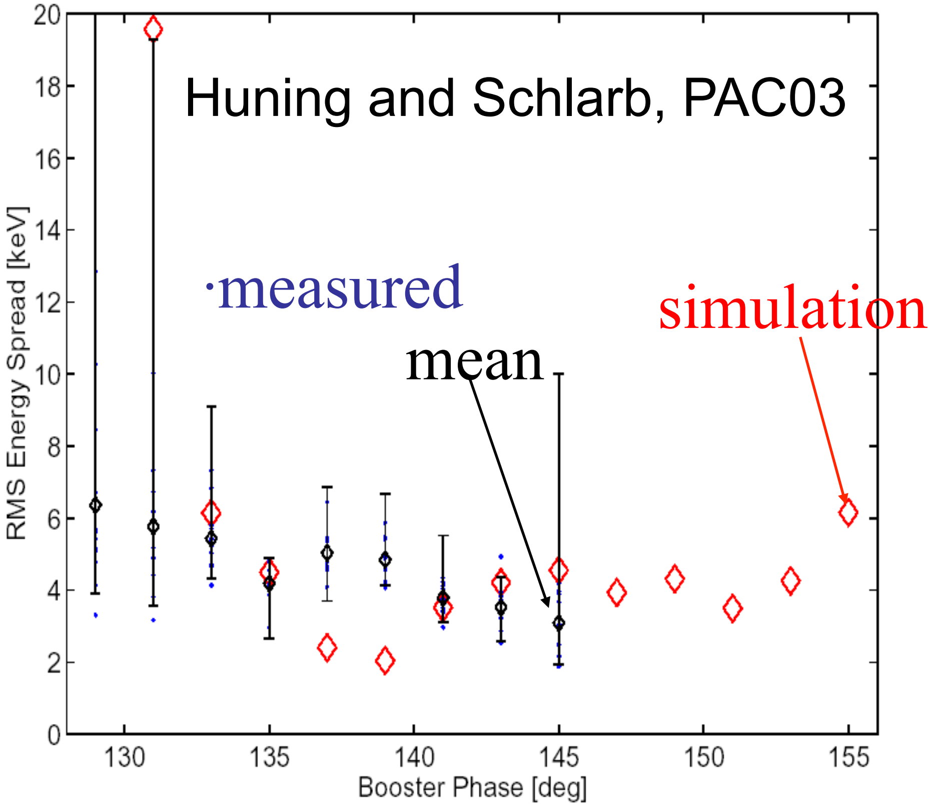

Instability mechanism

- Initial density modulation induces energy modulation through long. impedance Z(k), converted to more density modulation by a chicane ➔ growth of slice energy spread / emittance!

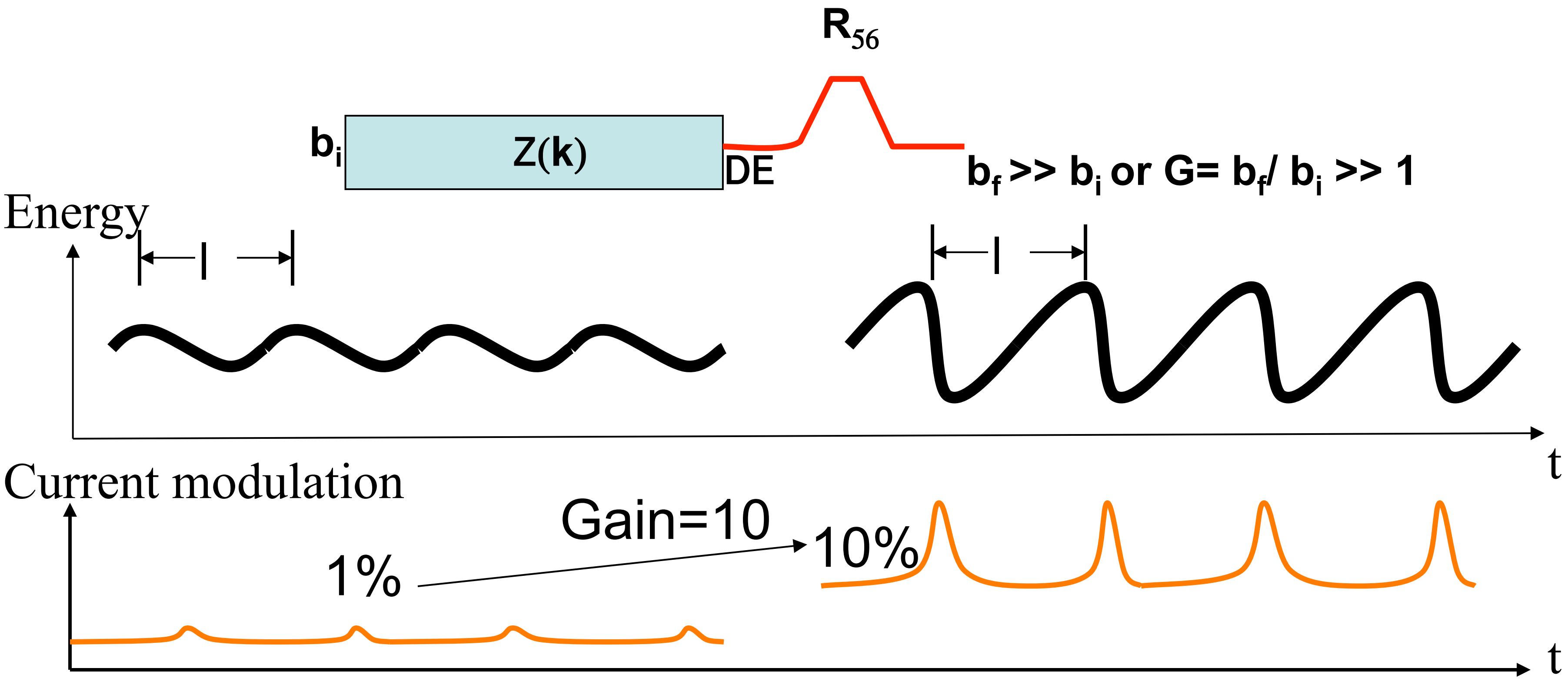

CSR Impedance

- Chicane introduces path length dependence on energy by bending the beam

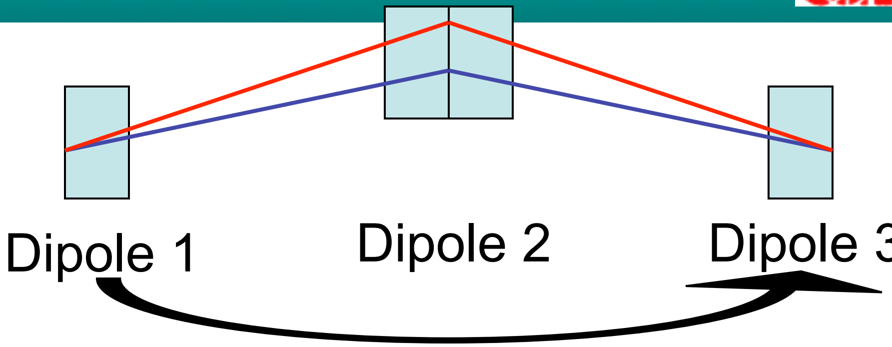

Dz=R$_{56}$ Dd

- Radiation from bunch tail catch up the head, increase energy spread and emittance

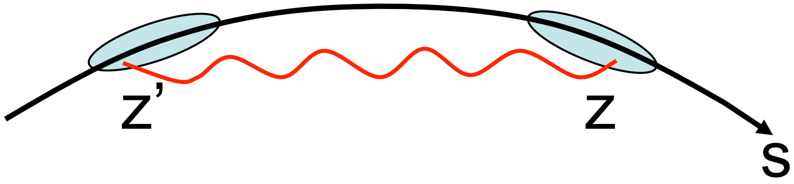

- CSR “wake” W(z-z’) or longitudinal impedance Z(k) (k =2p/l) (Murphy et al., Derbenev et al.)

$$\boxed{Z(k) = -iA\frac{k^{1/3}}{\rho^{2/3}}}$$

k =2p/l=w/c

Linac Impedance

- Linac wake (K. Bane)

$$W(s) \approx \frac{Z_0 c}{\pi a^2} e^{-\sqrt{s/s_0}}$$

***SLAC* S-Band:**

$s0$ 1.32 mm

a 11.6 mm

s < ~6 mm

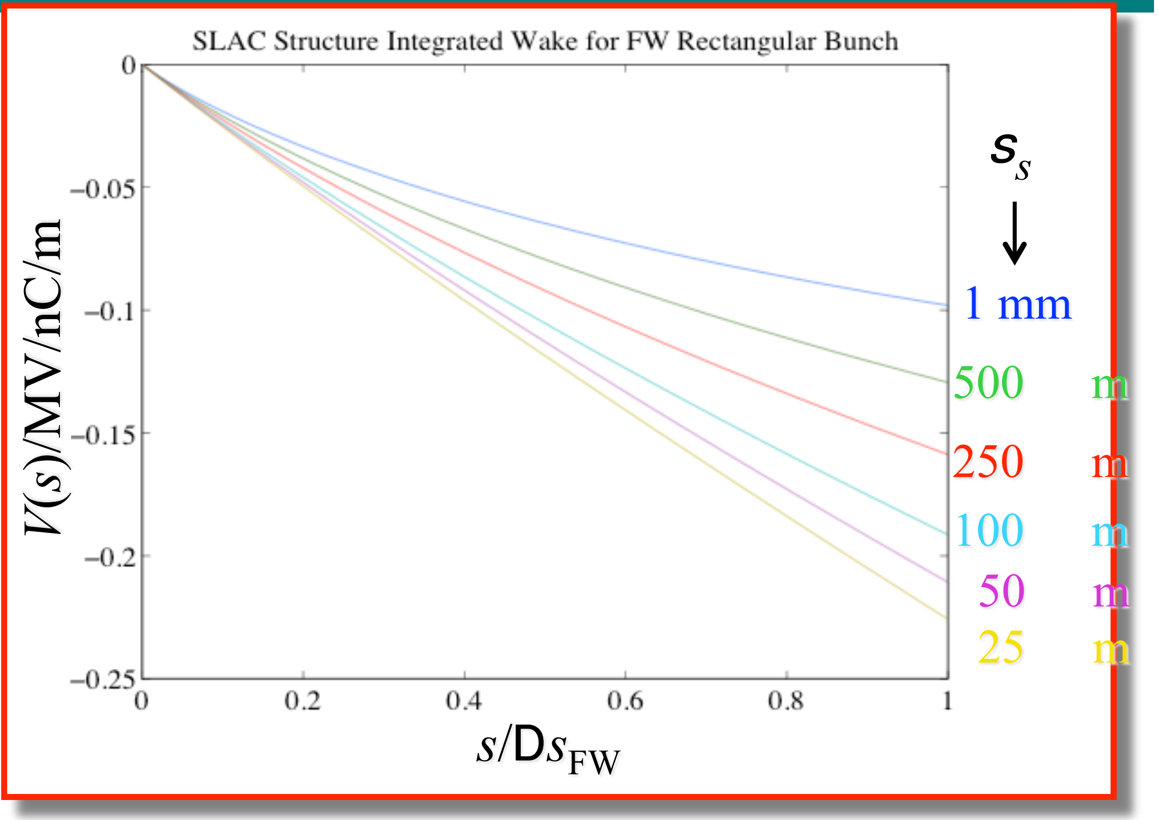

- To first order in 1/k

$$Z(k) = \frac{4i}{a^2 k} \quad \text{(capacitive)}$$

- Small at high frequency but can contribute to energy modulation over the entire linac (~1000 m)

LSC Impedance

- Free-space longitudinal space charge impedance

$$Z(k) = \frac{4i}{kr_b^2}\left[1 - \frac{kr_b}{\gamma}K_1\left(\frac{kr_b}{\gamma}\right)\right]$$

$$= \frac{4i}{kr_b^2} \text{ if } \frac{kr_b}{\gamma} \gg 1$$

$$= \frac{ik}{\gamma^2}\left(1 + 2\ln\frac{\gamma}{r_b k}\right) \text{ if } \frac{kr_b}{\gamma} \ll 1$$

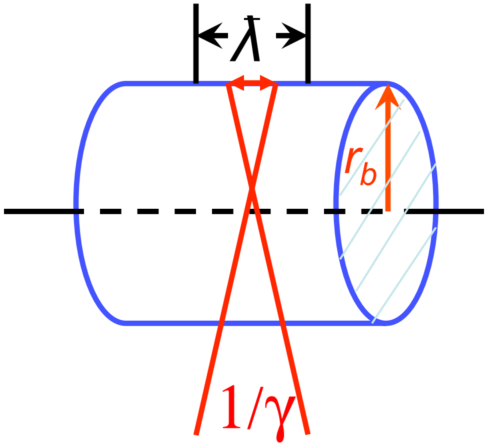

- At low energies inside the photoinjector, space charge oscillation dynamics (see J. Wu's talk)

- At higher linacs energy, beam density modulation freezes and energy modulation accumulates, dominant contribution at very high frequencies

Microbunching Gain

- Gain due to upstream impedances (LSC, linac wake)

$$G \equiv \left|\frac{b_f}{b_0}\right| = \frac{I_0}{\gamma I_A}\left|k_f R_{56} \int_0^L ds\, Z(k_0;s)\right| \exp\left(-\frac{1}{2}k_f^2 R_{56}^2 \underbrace{\sigma_\delta^2}_{\text{local energy spread}}\right)$$

- CSR microbunching

$$b_f(k;s) = b_0(k;s) + \underbrace{\underbrace{\int_0^s ds' K(s',s) b_0(k';s')}_{\text{one-stage amplification}}}_{I_f(1\to 3)+I_f(2\to 3)}$$

$$+ \underbrace{\underbrace{\int_0^s ds' K(s',s) \int_0^{s'} ds'' K(s'',s') b_0(k'';s'')}_{\text{two-stage amplification}}}_{I_f^2(1\to 2\to 3)}$$

Gain Curves

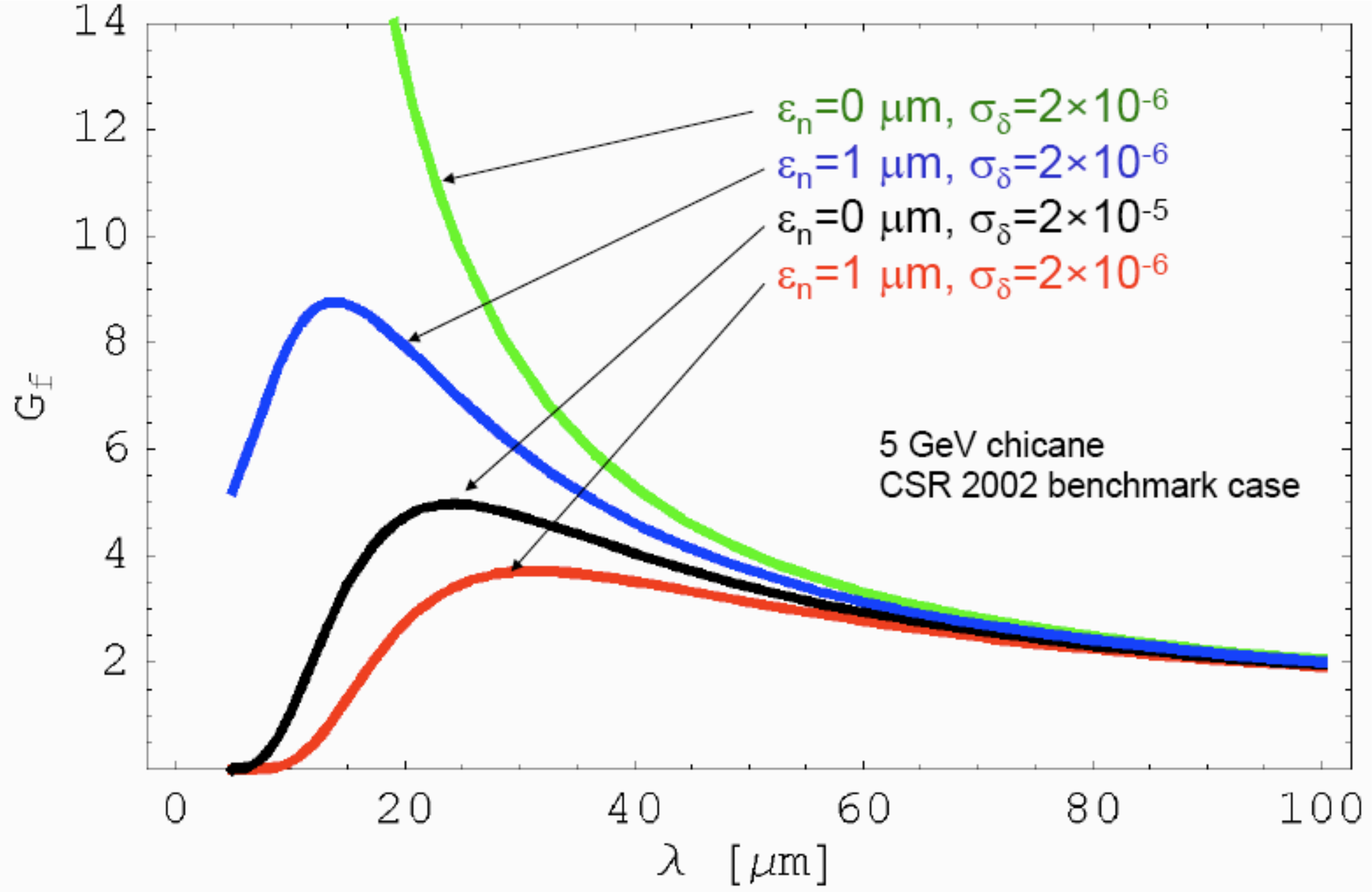
14
12
10
8
6
4
2
G_f
0
20
40
60
80
100
λ [μm]
ε_n=0 µm, $\sigma_\delta=2\times10^{-6}$
ε_n=1 µm, $\sigma_\delta=2\times10^{-6}$
ε_n=0 µm, $\sigma_\delta=2\times10^{-5}$
ε_n=1 µm, $\sigma_\delta=2\times10^{-6}$
5 GeV chicane
CSR 2002 benchmark case

LCLS Accelerator Systems

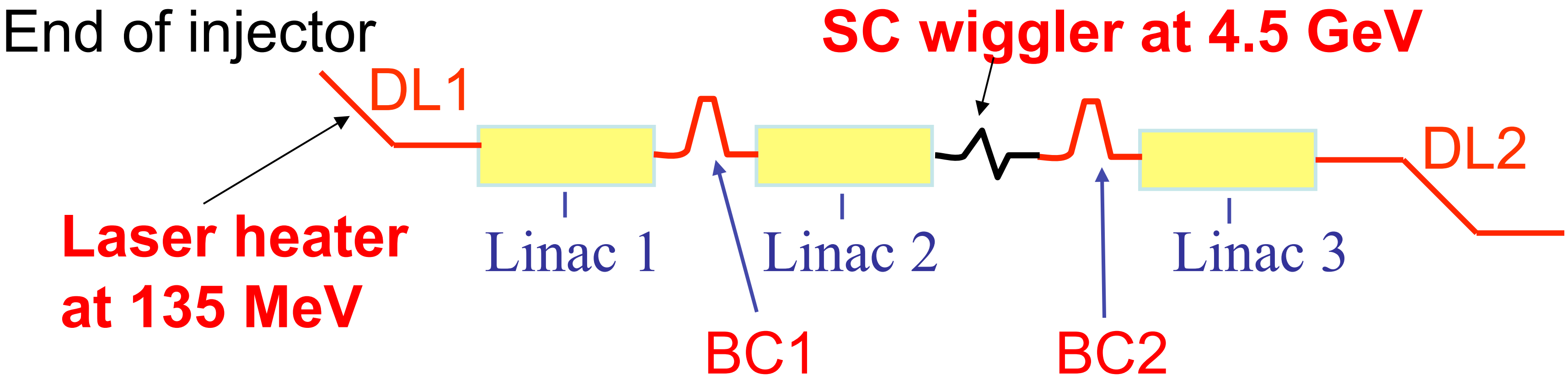

End of injector

SC wiggler at 4.5 GeV

DL1

DL2

Laser heater at 135 MeV

Linac 1

Linac 2

Linac 3

BC1

BC2

- At the end of injector, e-beam carries some residual density modulations which can be amplified in the downstream accel.

- Sources of impedance: CSR in dipoles, longitudinal space charge (LSC) and linac wakefields in linacs

- Landau damping options: a SC wiggler before BC2 at 4.5 GeV or a laser heater before DL1 at 135 MeV

Allowable Laser Heating

- FEL parameter $r \sim 5\times10^{-4}$, not sensitive to energy spread until $s_d \sim 1\times10^{-4}$

M. Xie's fitting formula
ge = 1.2 mm
I_p = 3.4 kA
b = 20 m

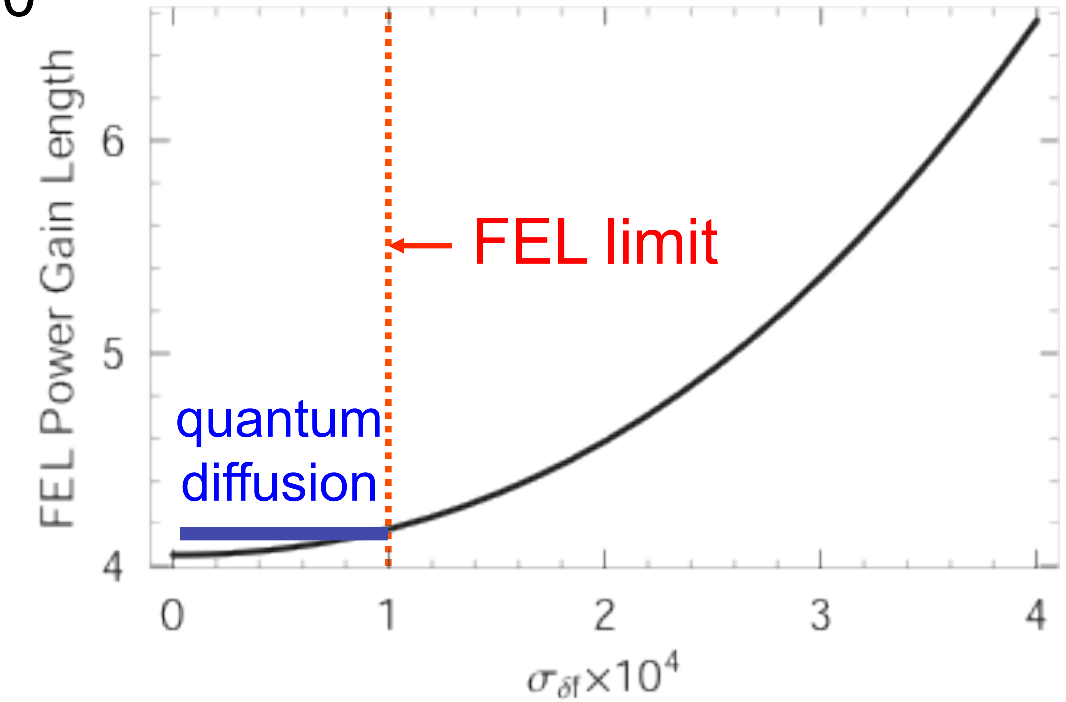

- 3 keV initial energy spread after compression = 90 keV, corresponding to $s_d < 1\times10^{-5}$ at 14 GeV

➔ can increase s_d by a factor of 10 without FEL degradation

Laser Heater

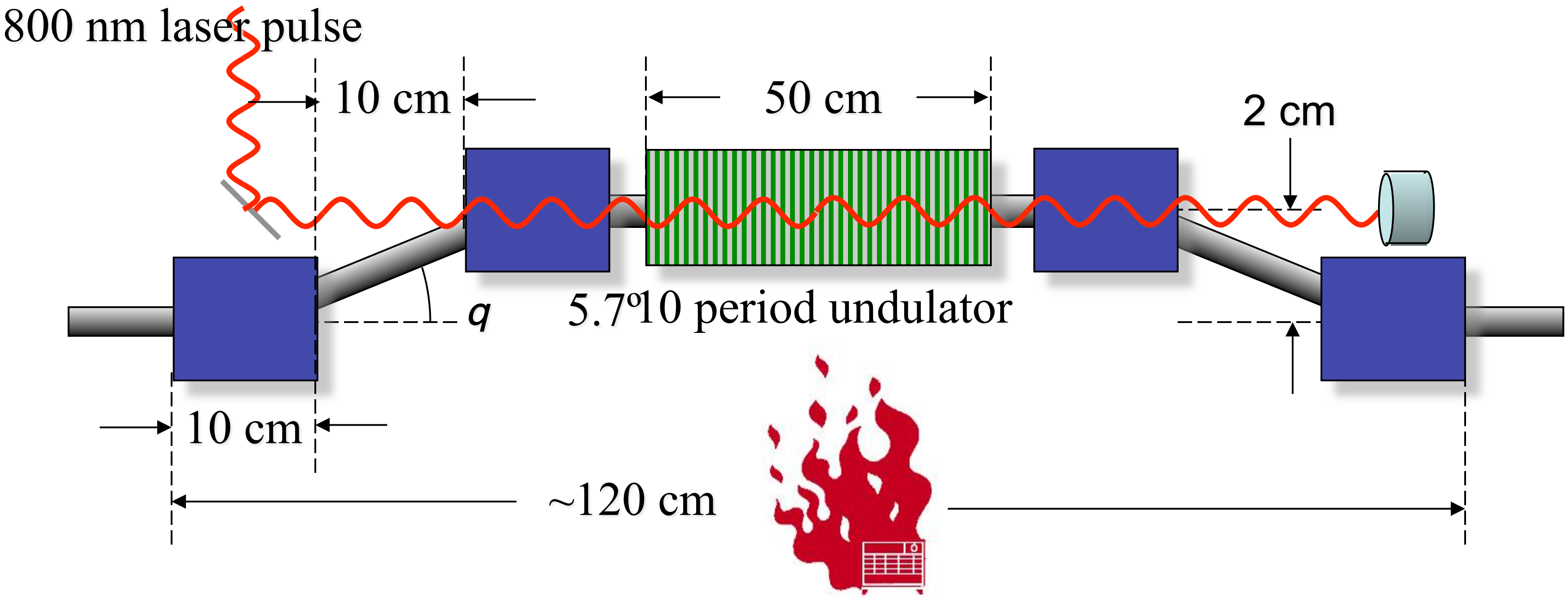

- Laser-electron interaction in an undulator induces rapid energy modulation (at 800 nm), to be used as effective energy spread before BC1 (3 keV➔ 40 keV rms)

- Inside a weak chicane for easy laser access, time-coordinate smearing (emittance growth is completely negligible)

Simulation of Laser Heating

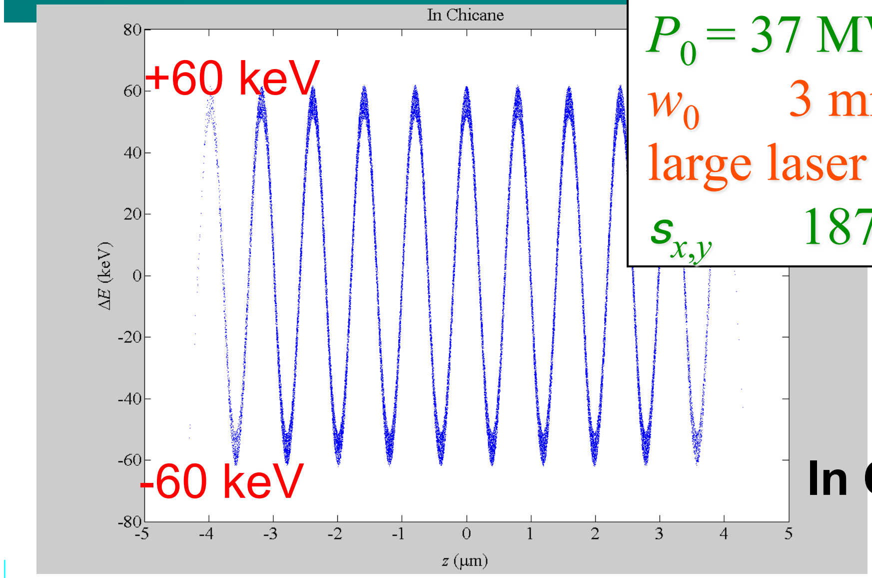

$P_0 = 37$ MW
w_0 3 mm
large laser spot
$s_{x,y}$ 187 *m*m

In Chicane

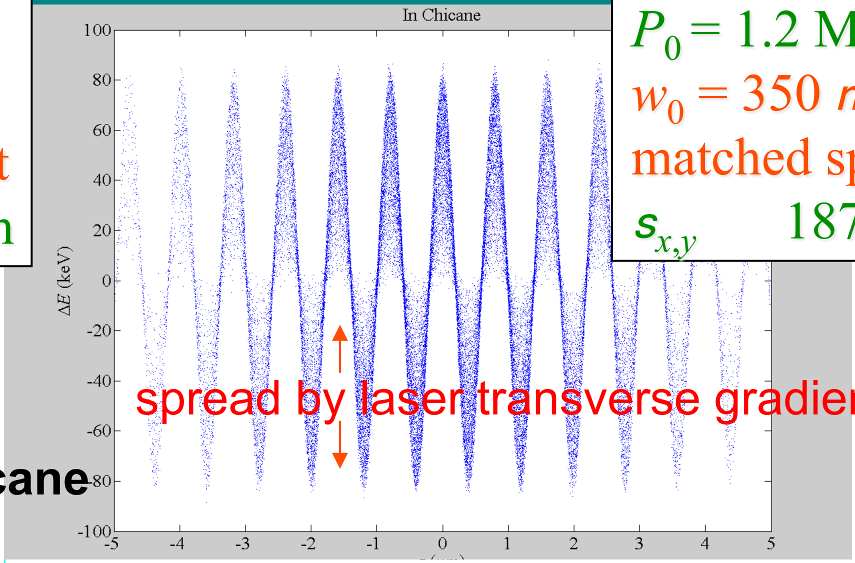

$P_0 = 1.2$ MW
$w_0 = 350$ *m*m
matched spot
$s_{x,y}$ 187 *m*m

spread by laser transverse gradient

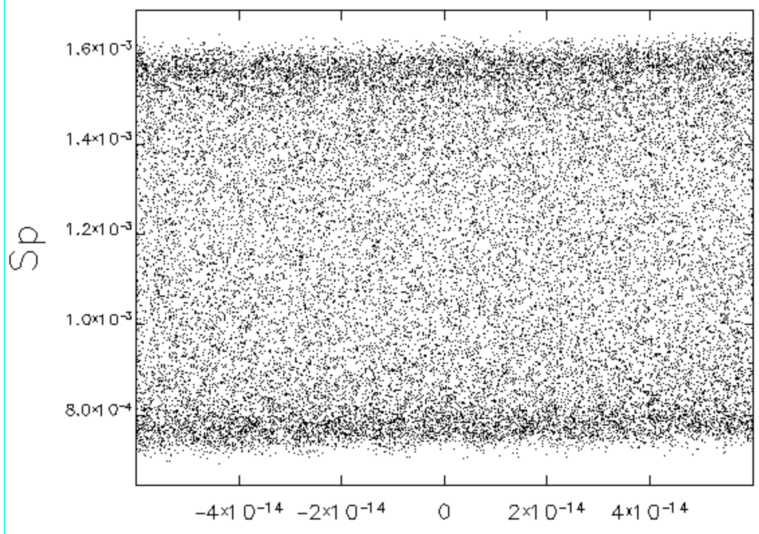

After Chicane

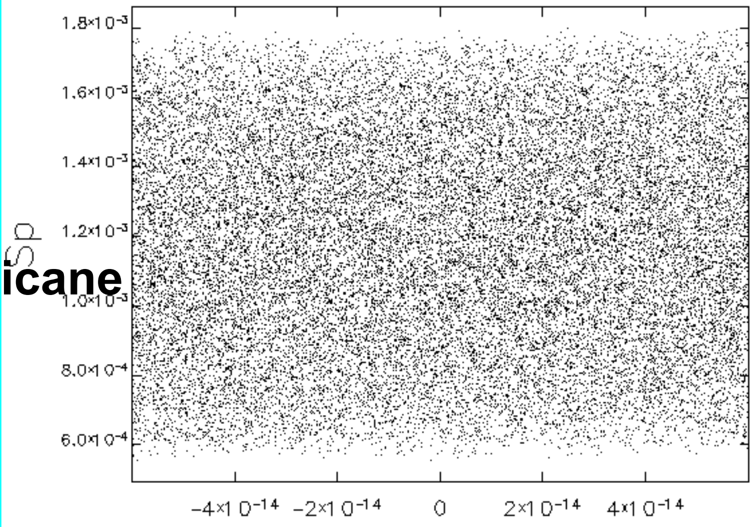

Non-uniform heating

more uniform heating

Dependence on laser spot size

- Large laser spot generates “double-horn” energy distributioin, ineffective at suppressing short wavelength microbunching
- Laser spot matched to e-beam size creates better heating

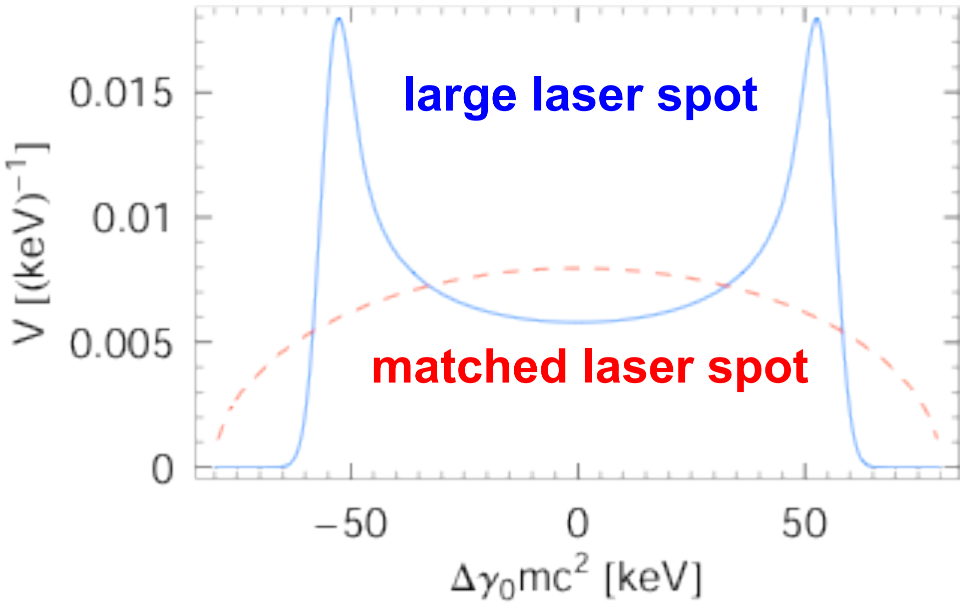

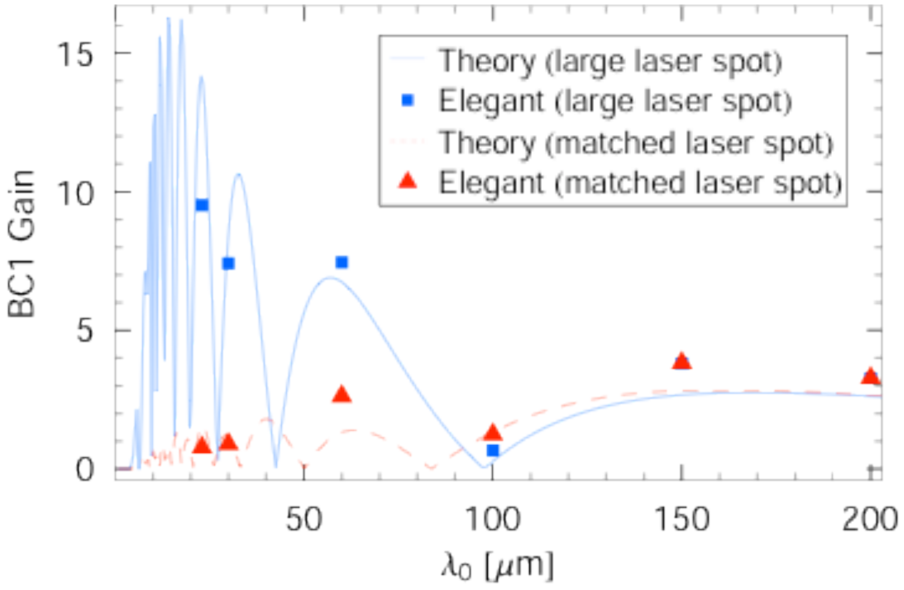

$$\frac{G_L}{G_0} = J_0(k_f R_{56}\delta_L) \sim (k_f R_{56}\delta_L)^{-1/2} \text{ when } \sigma_r \gg \sigma_x$$

$$\frac{G_L}{G_0} = 2\frac{J_1(k_f R_{56}\delta_L)}{k_f R_{56}\delta_L} \sim (k_f R_{56}\delta_L)^{-3/2} \text{ when}$$

Net effect for LCLS

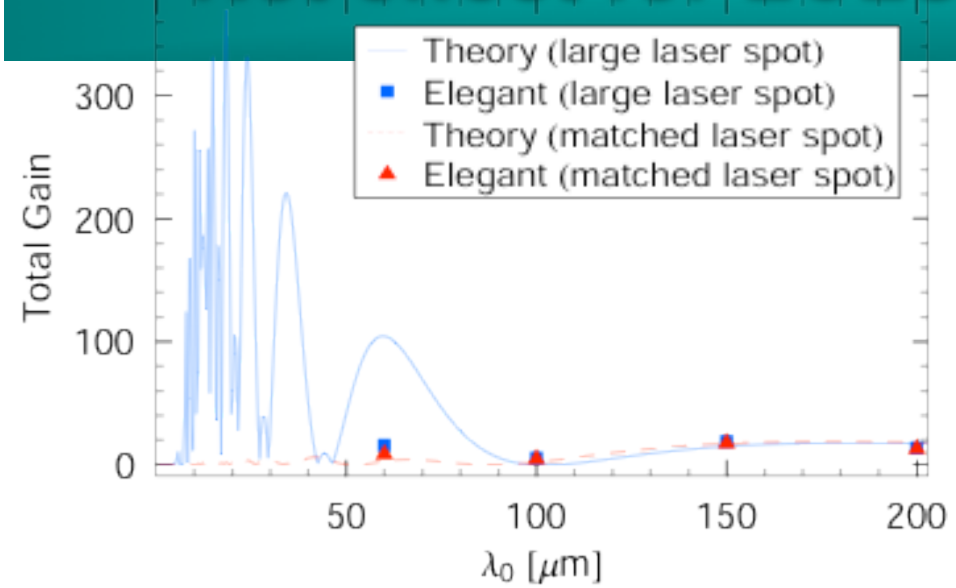

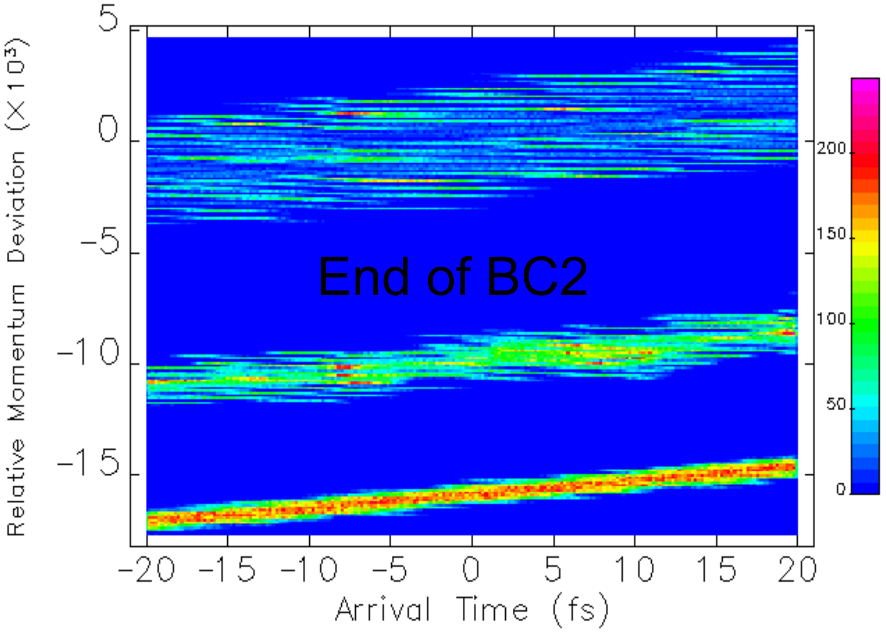

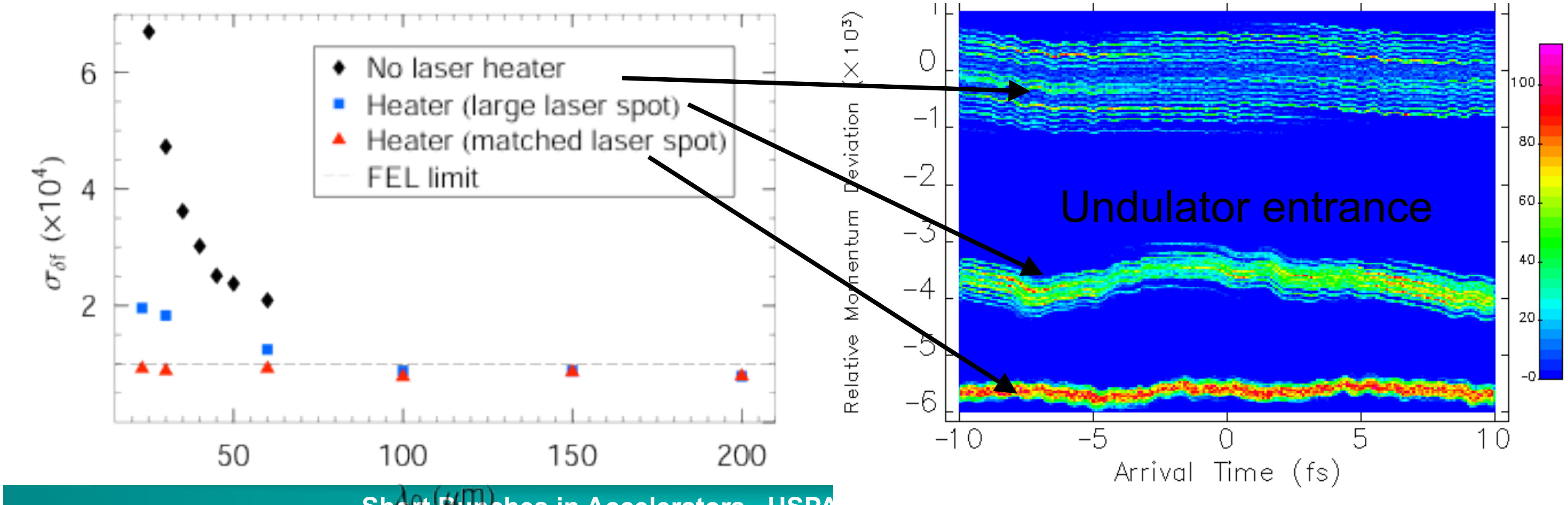

Injector Longitudinal Phase Space

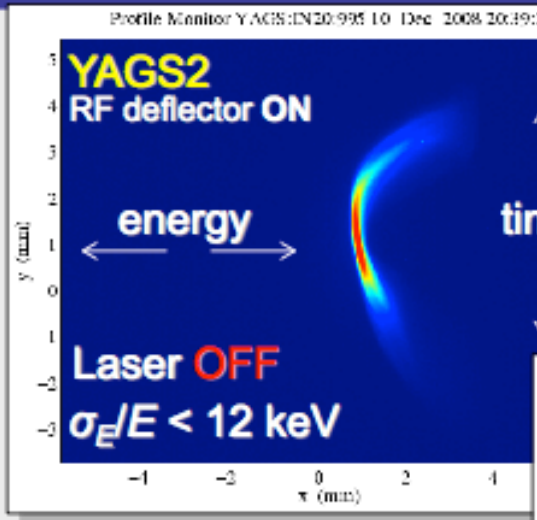

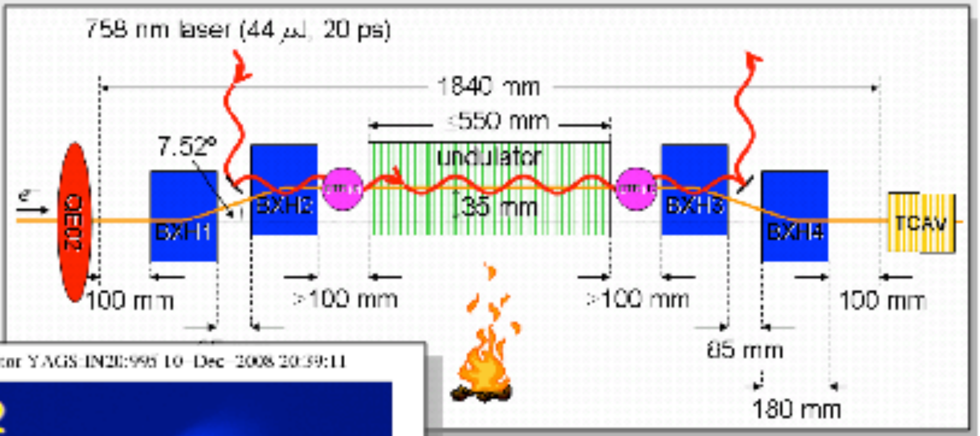

Dec. 10, 2008

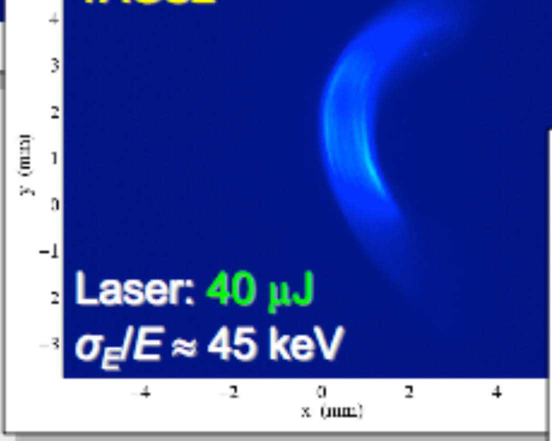

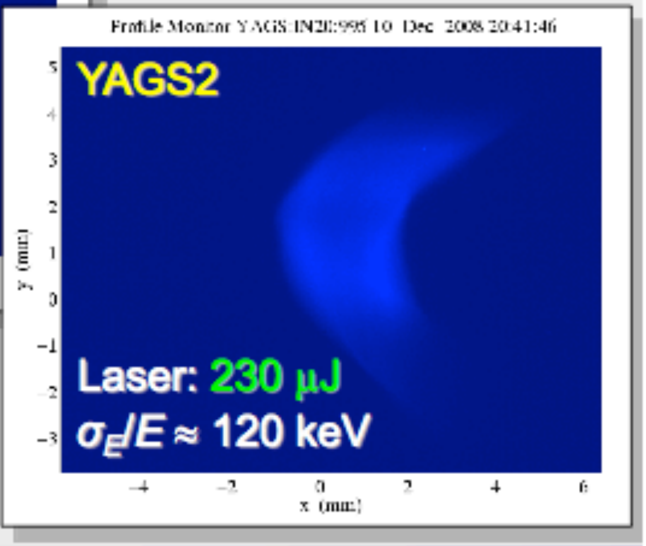

Laser heater effect on slice energy spread can be studied

Timing between heater laser & electron beam adjusted

COTR from Microbunching in LCLS: Measurements

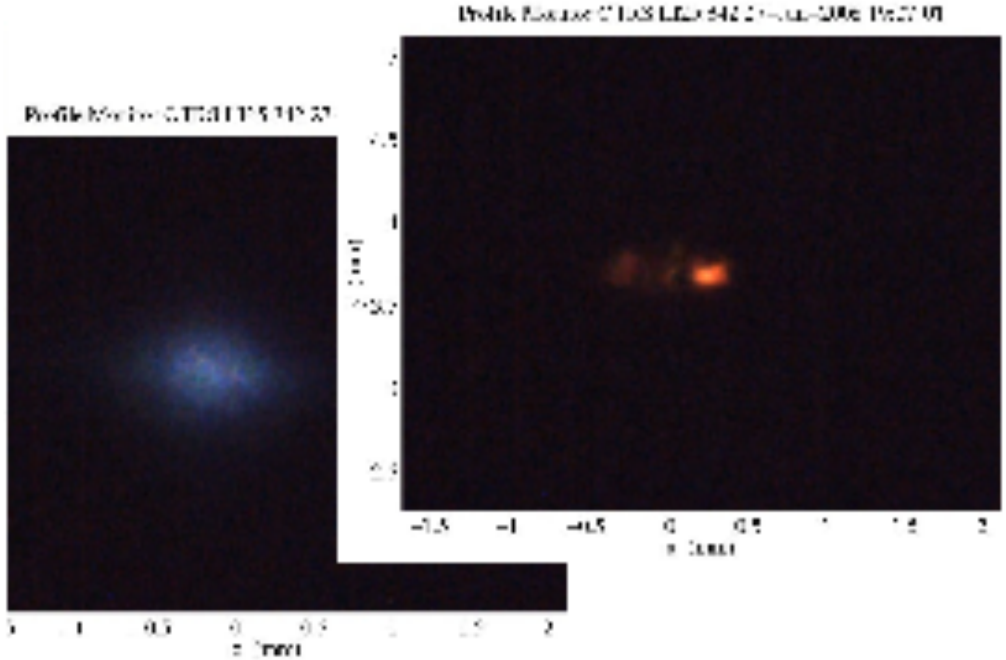

10,000X enhanced COTR

COTR makes OTR screens useless above 250 MeV

Coherent OTR light does not appear to have the same transverse distribution as incoherent OTR.

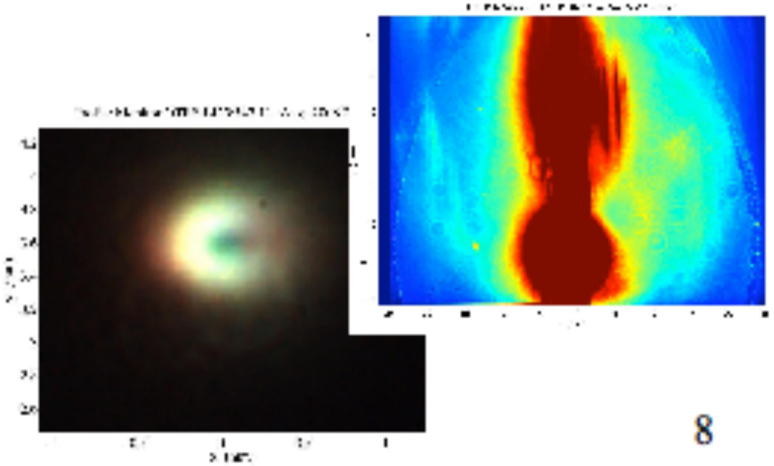

COTR from Microbunching in LCLS: Measurements

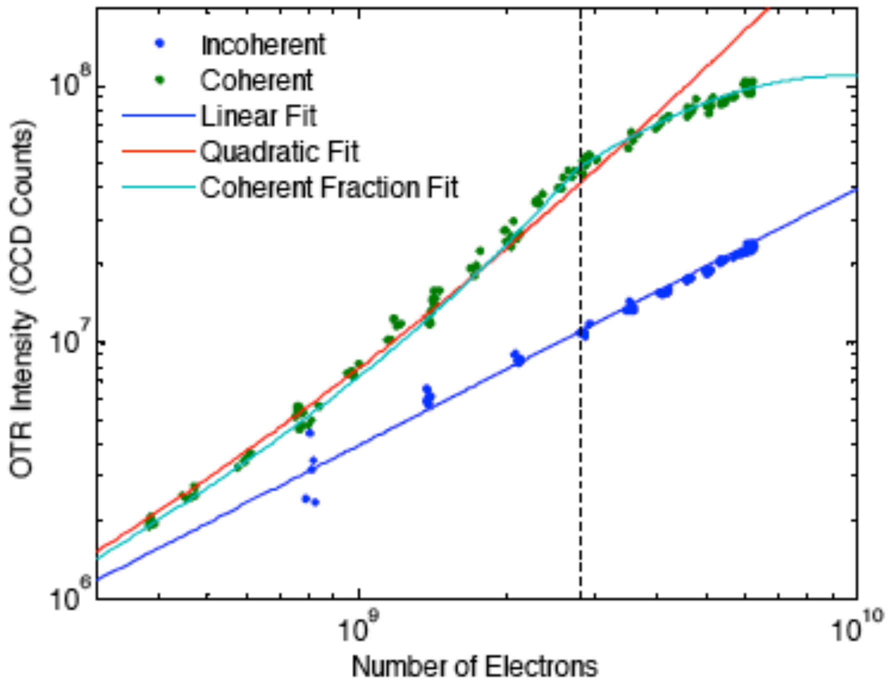

Figure 4: Dependency of OTR light intensity on the bunch charge. The data shown is for 250 MeV and uncompressed bunches. The coherent fraction fit uses the fit from Fig. 5.

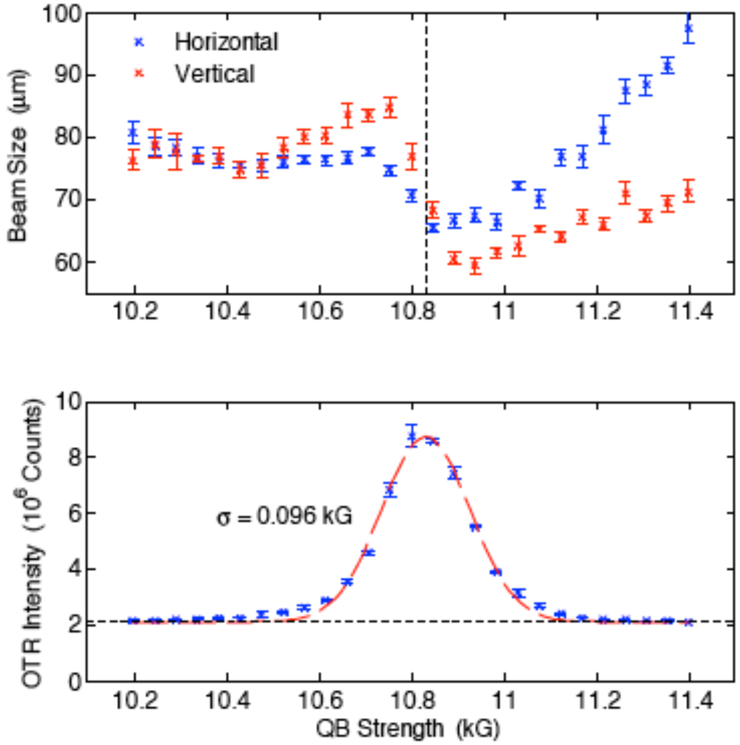

Figure 3: OTR intensity (lower) and beam sizes (upper part) measured downstream of BC1 at OTR12 as a function of the dispersion correction quadrupole (QB) in the first dogleg with no bunch compression. The vertical line indicates the peak of the OTR intensity curve.

SDL zero-phasing observation

(W. Graves et al.)

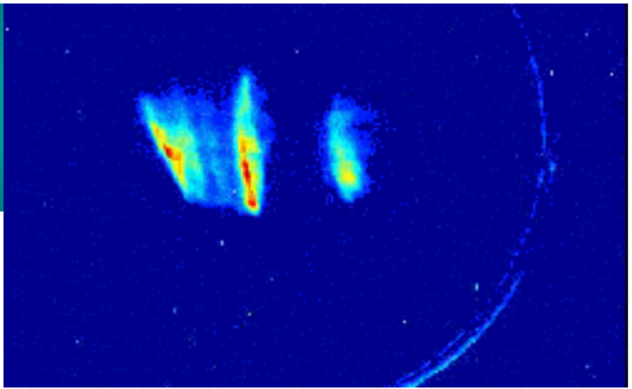

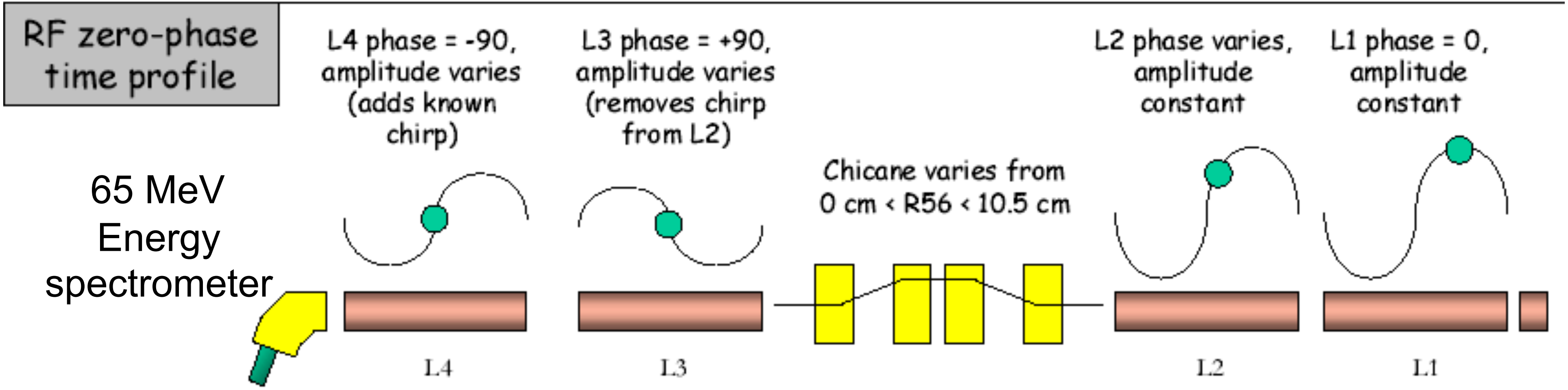

RF zero-phase time profile

L4 phase = -90, amplitude varies (adds known chirp)

L3 phase = +90, amplitude varies (removes chirp from L2)

Chicane varies from 0 cm < R56 < 10.5 cm

L2 phase varies, amplitude constant

L1 phase = 0, amplitude constant

65 MeV Energy spectrometer

X (E) profile

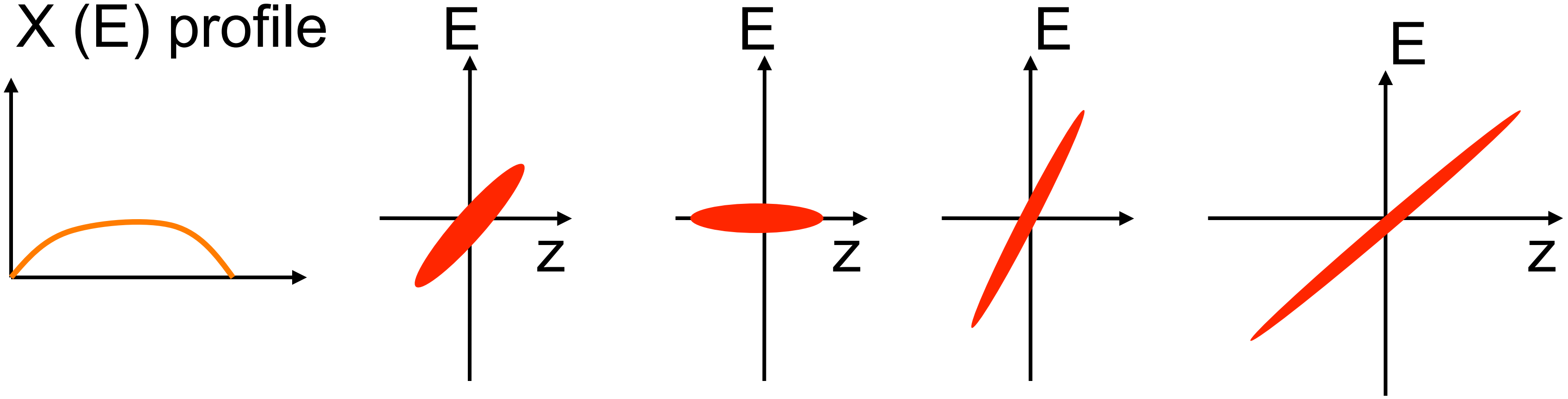

Sensitive to energy modulation

- rf zero phasing energy spectrum is very sensitive to beam energy modulation

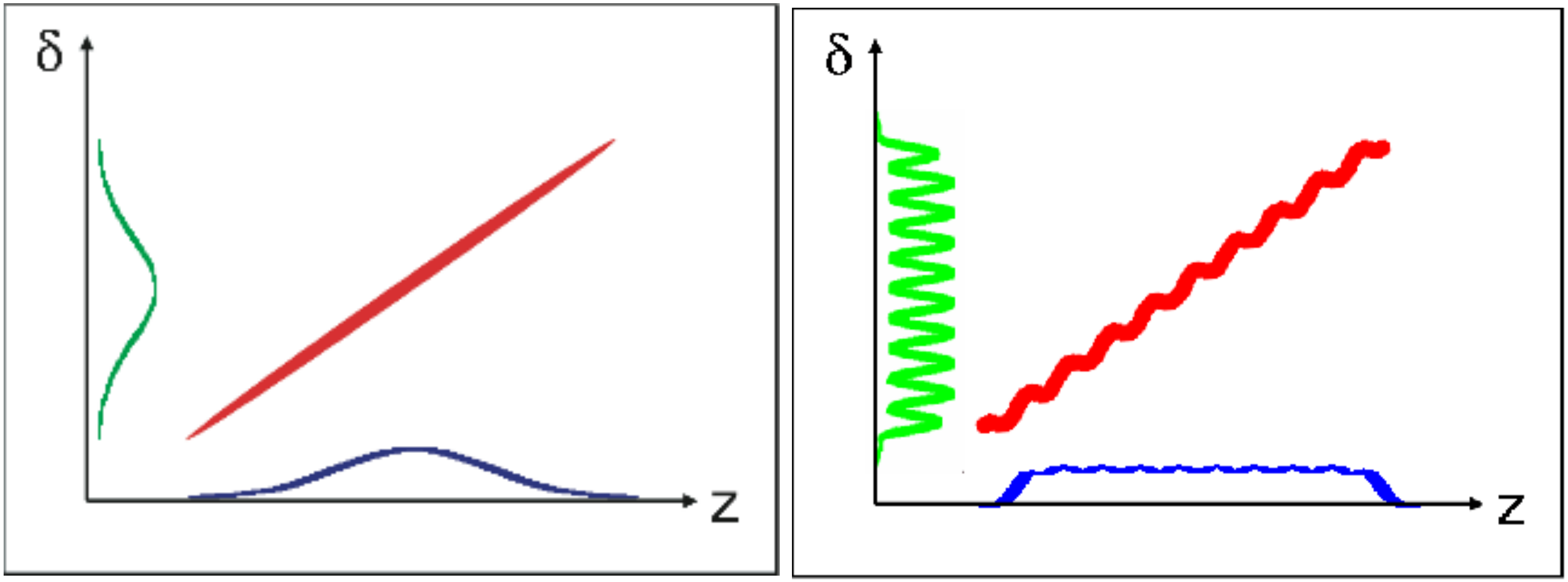

- Small energy modulation gets projected to large horizontal density modulation (enhanced by I_{rf}/I_m ~ 1000)
- Measurement can be used to reveal energy modulations

Beam size dependence

- “Zero-phasing” profiles of the beam (300 pC) for different lattice solutions: (Shaftan et al.)

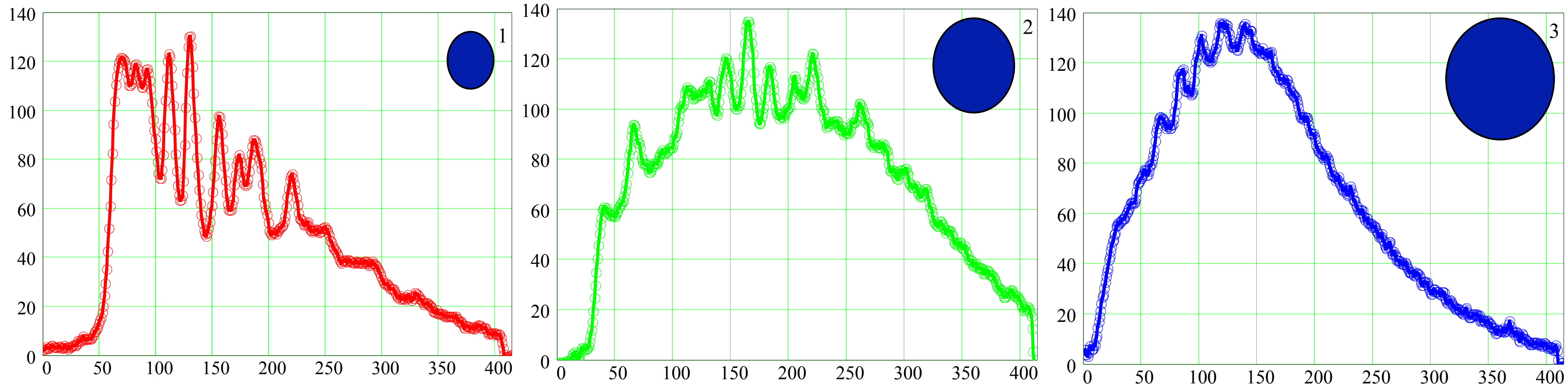

Average RMS beam sizes along the accelerator: 0.25 mm, 0.5 mm, 1 mm

- Model: energy modulation induced by LSC (depend on r_b)

$$\left[\frac{\gamma I_0}{I_A}\frac{\lambda Z_{LSC}(r_b,\lambda)}{2\pi}\right]^{1/2} b_i \sin\left(\frac{\Omega_{SC}L}{c}\right)$$

SC oscillation freq.

$$\Omega_{SC} = c\sqrt{\frac{2\pi I_0}{\gamma^3 I_A}\frac{|Z_{LSC}|}{\lambda}}$$

Modulation wavelength

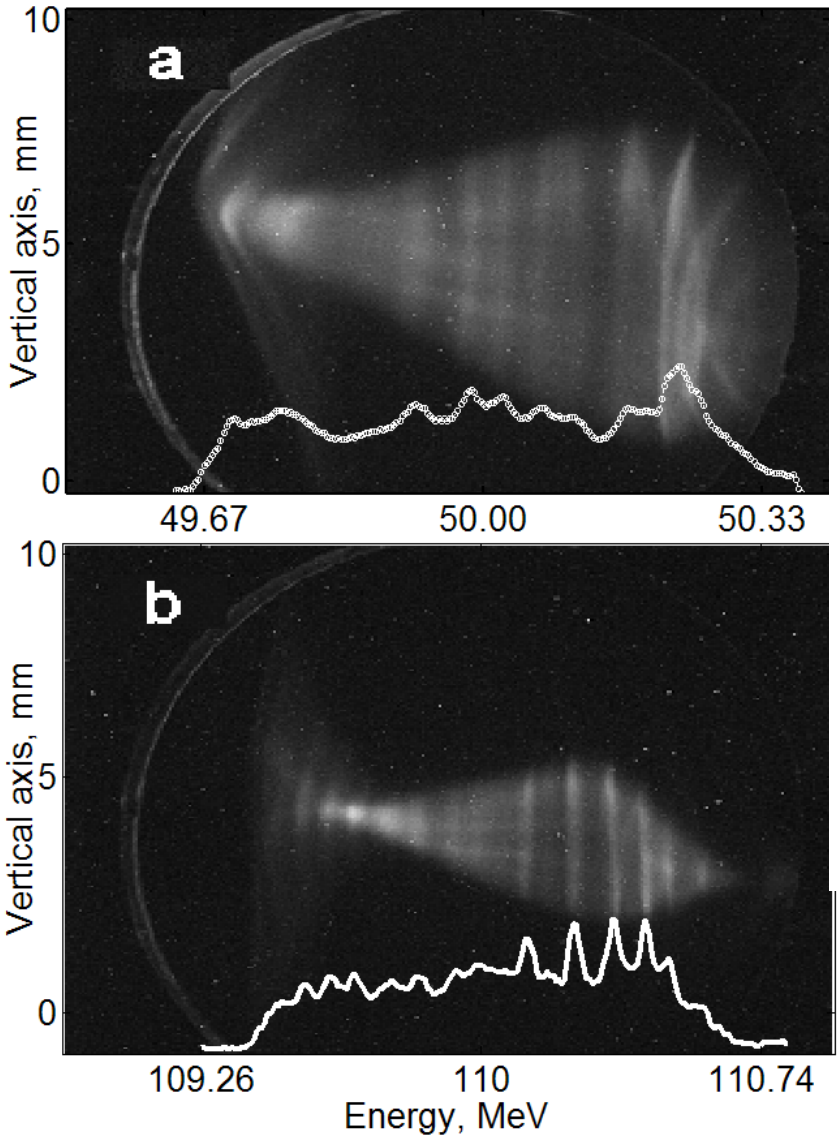

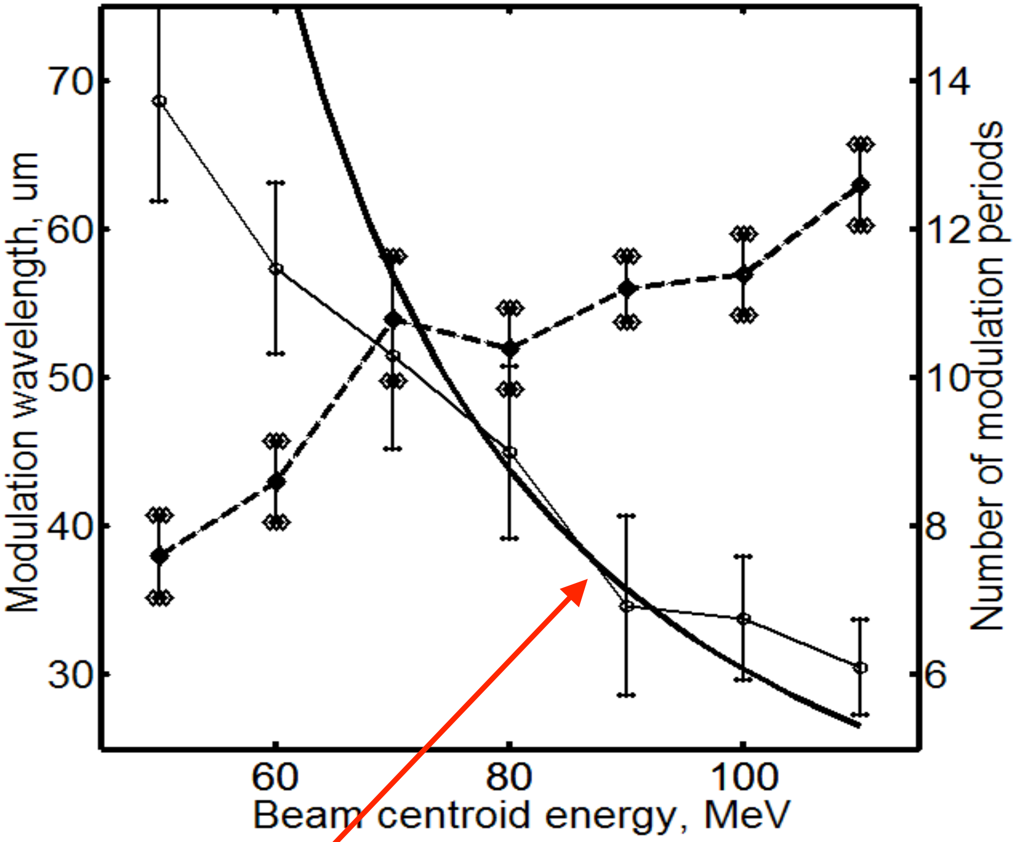

Wavelengths correspond to calculated maximum energy modulation

Elegant Simulation of MBI

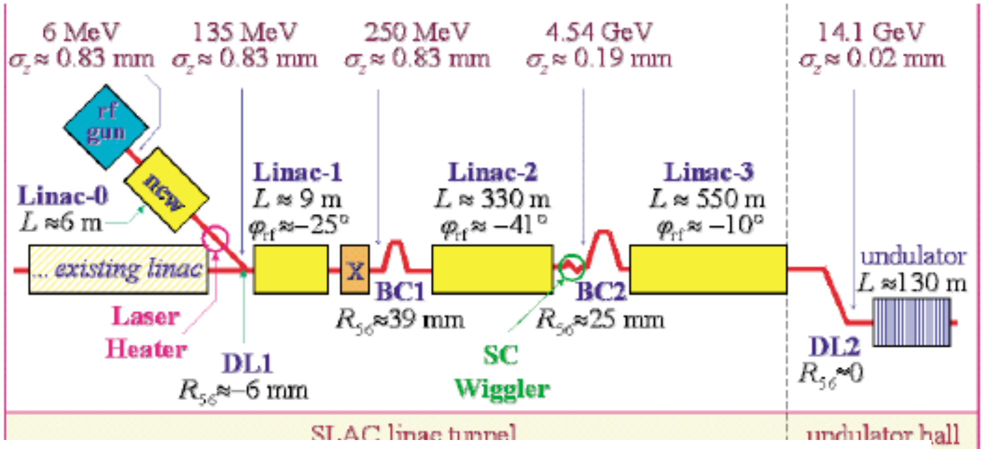

λ=15μm: Initial Distribution

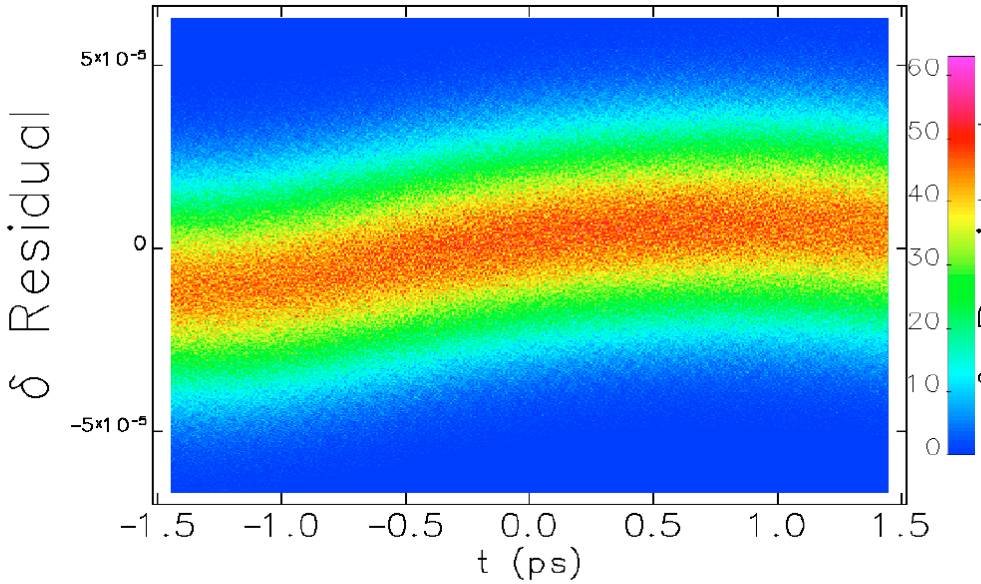

λ=15μm: BC1 Entrance

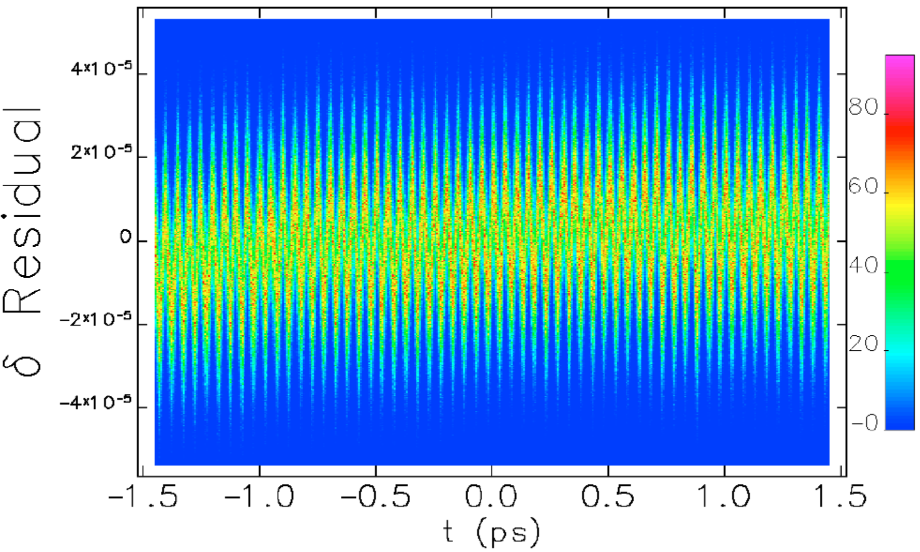

Elegant Simulation of MBI

λ=15µm: BC1 Exit

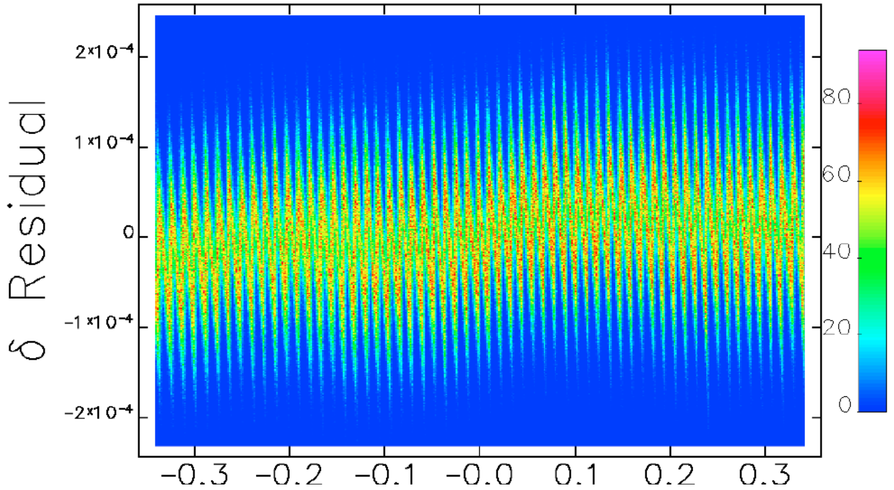

λ=15µm: BC2 Entrance

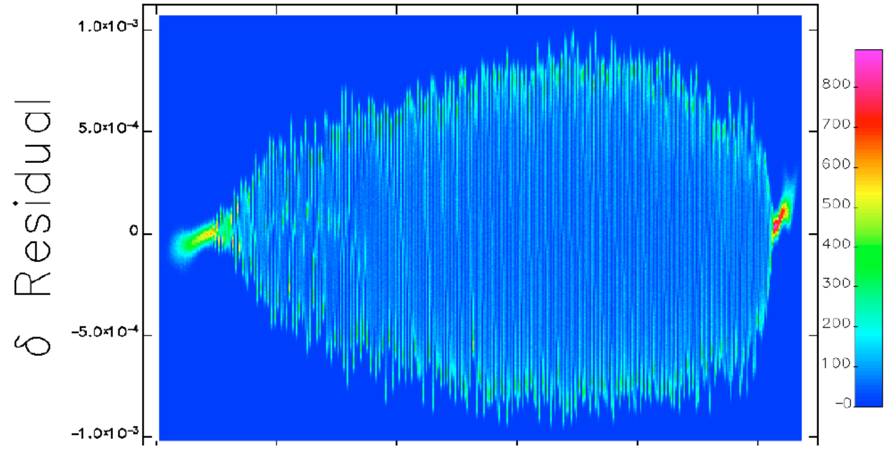

λ=15µm: BC2 Exit

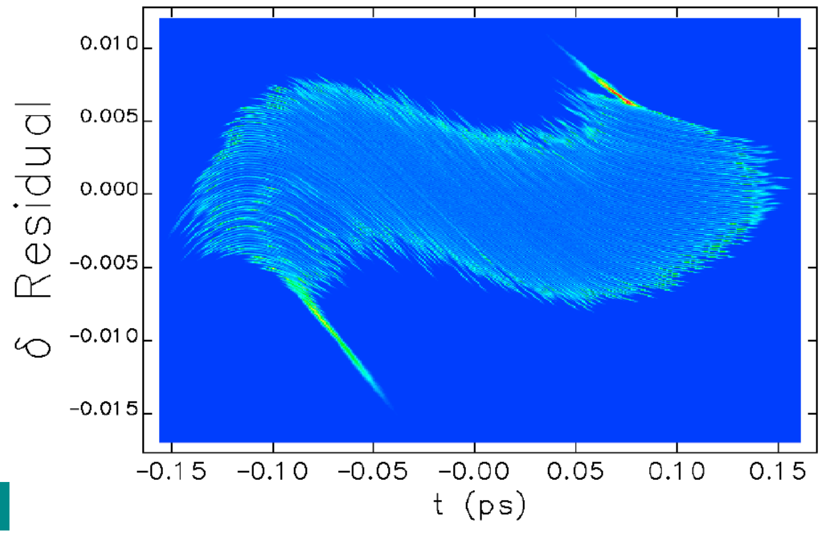

λ=15µm: DL2 Exit

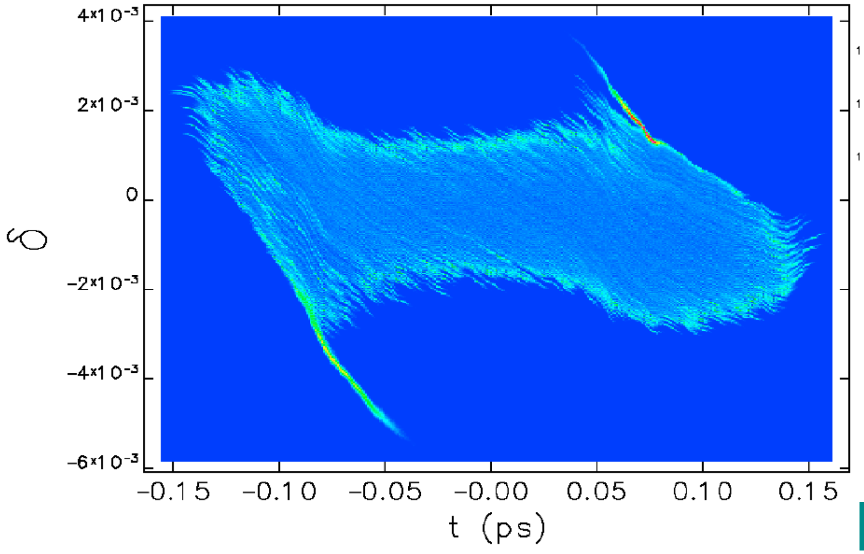

Elegant Simulation of MBI

λ=60μm: DL2 Exit

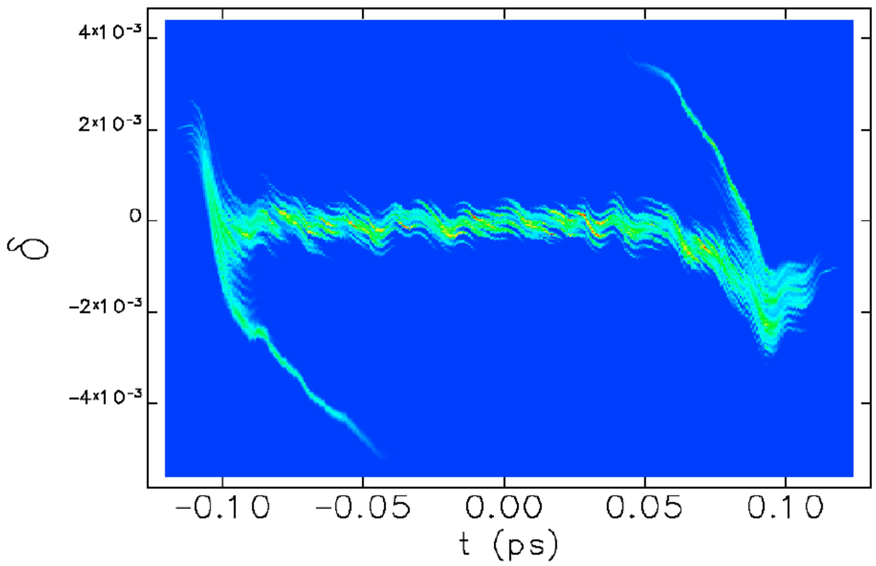

λ=200μm: DL2 Exit

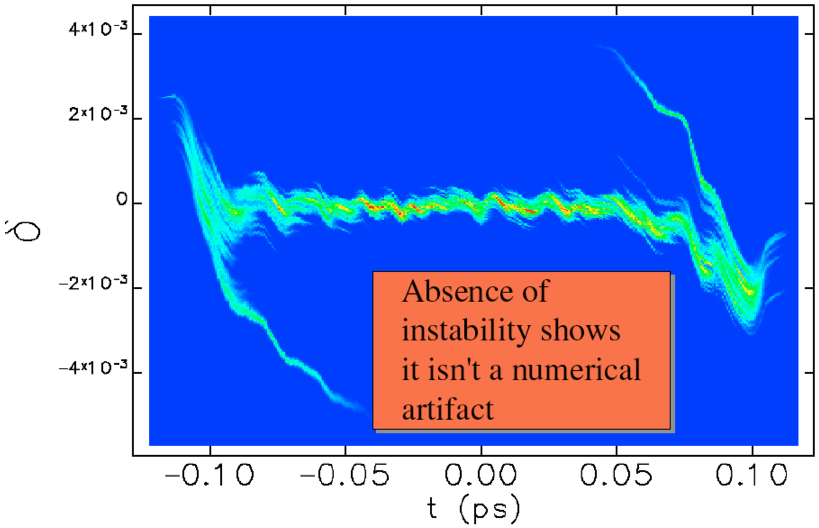

Absence of instability shows it isn't a numerical artifact

Further developments on simulation of MBI

Starts from a shot noise, produces chaotic variations to the energy and peak current, incredibly difficult to model

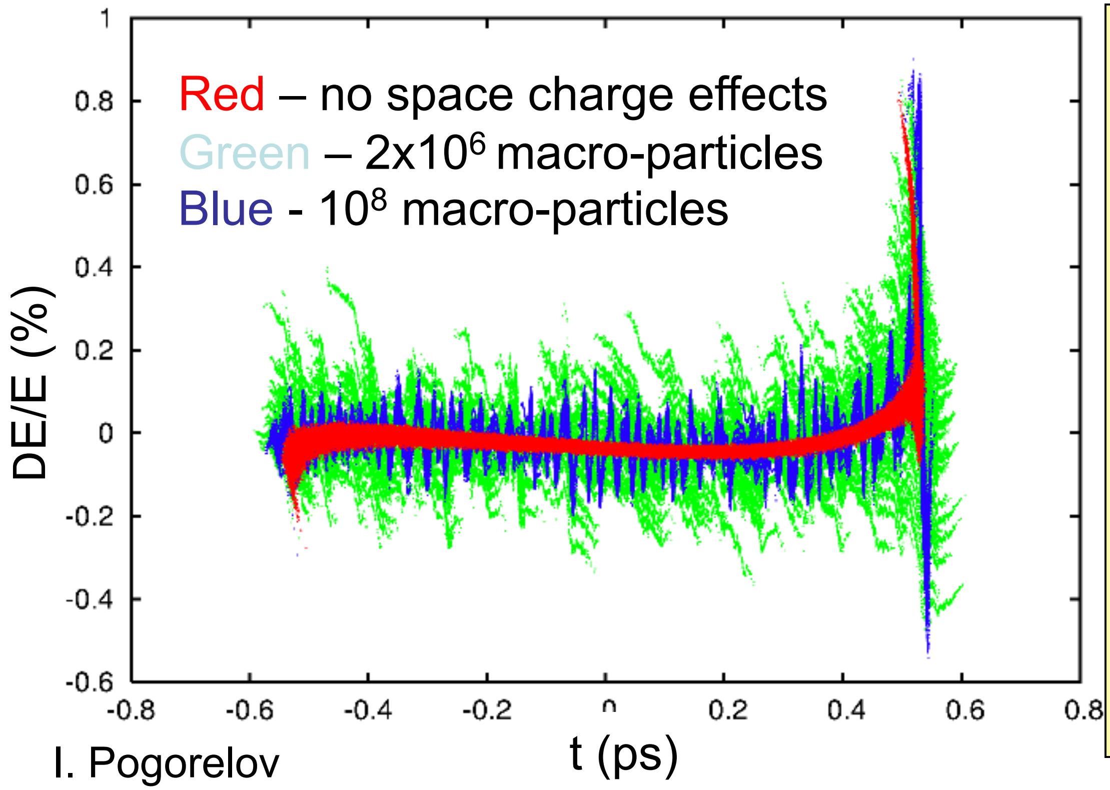

I. Pogorelov

simulated with **IMPACT**

1) Particle loading:

global fitting, re-sampling in 6D, quiet start

2) Grid selection:

grid noise, resolving “hidden” correlations, minimize computational time

2) Lumped space-charge and wakefield kicks to speed up simulation

J. Qiang, W. Fawley, M. Venturini

Revealing “true” physics over the numerical noise

Summary of single pass effects

- Microbunching instability driven by LSC, CSR and machine impedance can be a “nightmare” for x-ray FELs
- The photoinjector beam is too “cold” in energy spread, “heating” within the FEL tolerance (~10X) can damp the instability without affecting the FEL gain
- A laser heater with a laser spot matched to the transverse e-beam size can effectively suppress microbunching
- SDL “microbunching” is dominated by LSC-induced energy modulation in the linac
- With a stronger dispersion section, the modulator can be used as a laser heater to suppress the microbunching gain

Compare Linac and Ring MBI

- CSR interaction and physics identical to single pass MBI. Space charge typically insignicant for rings.
- Storage ring peak currents typically much smaller (1 nC/30 psec)
- Storage have longitudinal oscillations (synchrotron) which tend to mix instabilities
- Effective arc length in rings >>> than single pass.

CSR MBI

CSR can drive a microbunching instability in the electron bunch, resulting in a periodic bursts of terahertz synchrotron radiation, resulting in a noisy source.

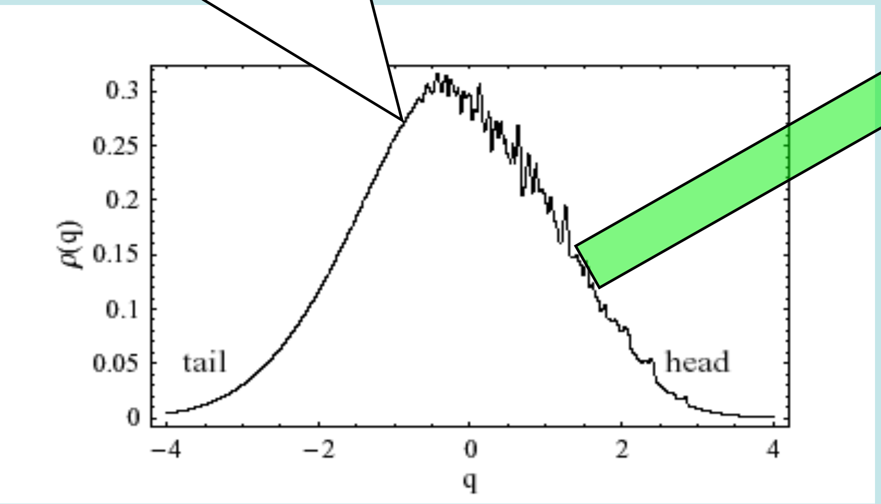

Simulated instability showing bunch modulation
M. Venturini, R. Warnock, PRL **89**, 224802, (2002).

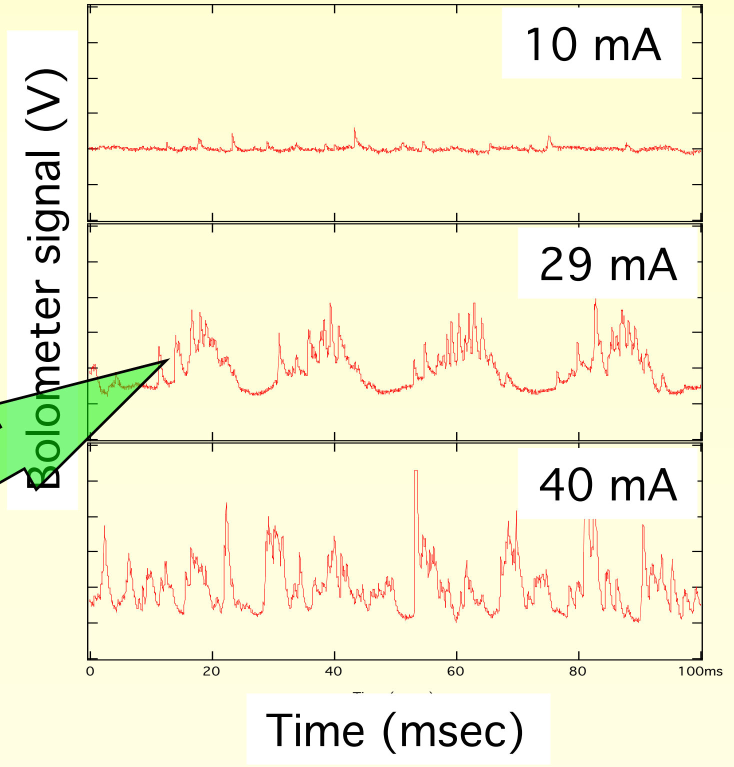

Bursts of far-IR CSR observed on a bolometer. Threshold depends on beam energy, bunch length, energy spread, and wavelength.

Linear Stability Analysis

Instability theory is well-developed for synchrotrons. Use linearized Vlasov approach to calculate instability threshold using radiation impedance. Accounts for damping from energy spread (Landau damping)

- Linearized Vlasov equation comes from conservation of phase space density
  - does not include damping mechanism (radiation damping)
  - does not include noise excitation (quantum excitation)

$$\frac{\partial f_1}{\partial t} + p\frac{\partial f_1}{\partial q} + I\omega_0\frac{\partial f_0}{\partial p} \times$$
$$\frac{1}{2\pi}\sum_{n=-\infty}^{\infty} Z(n)e^{iq\sigma_z/R}\int e^{-iq\sigma_z/R}\rho_1(q)dq = 0.$$

Assume a single mode excitation

$$f_1 = \hat{f}_1(p)\exp[-i(\nu\theta - nq\sigma_{z0}/R)]$$

$$iI\omega_0\frac{Z(n)}{n}\left(\frac{R}{\sigma_z}\right)^2\int_{-\infty}^{\infty}\frac{\partial f_0/\partial p}{p-\nu R/\sigma_z n}dp = 1,$$

Radiation Impedance with cutoff

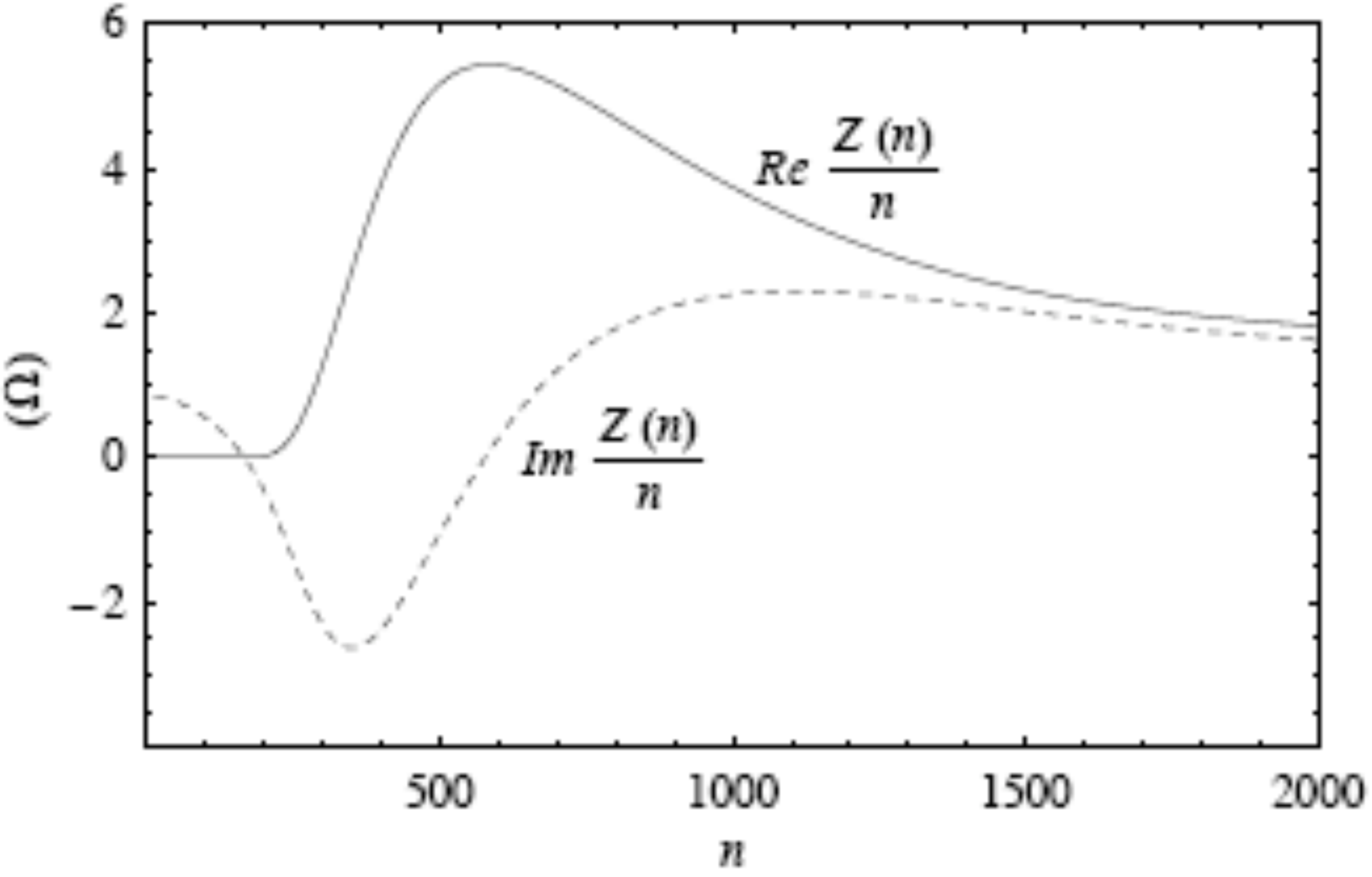

Stability Criterion

$$-\frac{I\omega_0}{\sqrt{2\pi}}\left(\frac{R}{\sigma_z}\right)^2\frac{Z(n)}{n}=-\frac{i}{W_D(\nu R/\sigma_z n)}$$

Yields stability threshold (Im □>0)

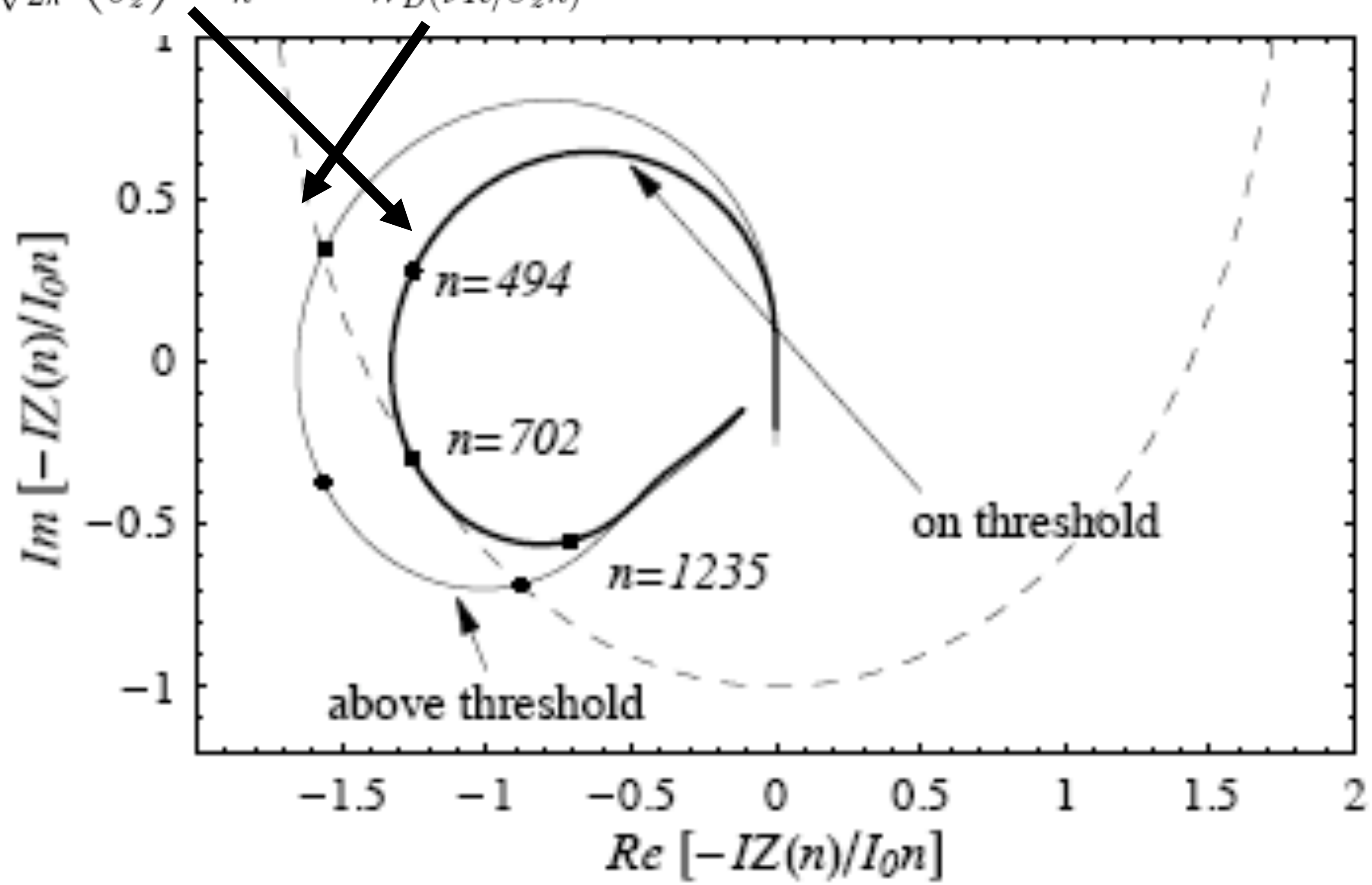

Bessy-II Microbunching

Single bunch CSR-signal at 1.25 MHz and ~5Hz bandwidth

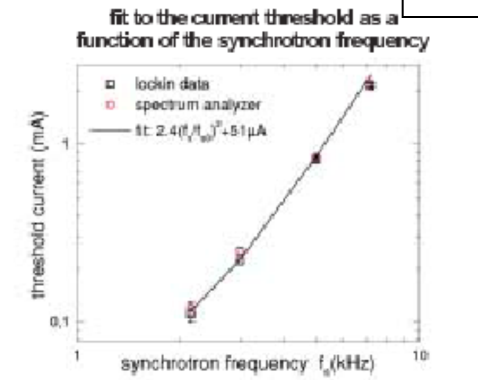

Agrees well with predicted microbunching thresholds

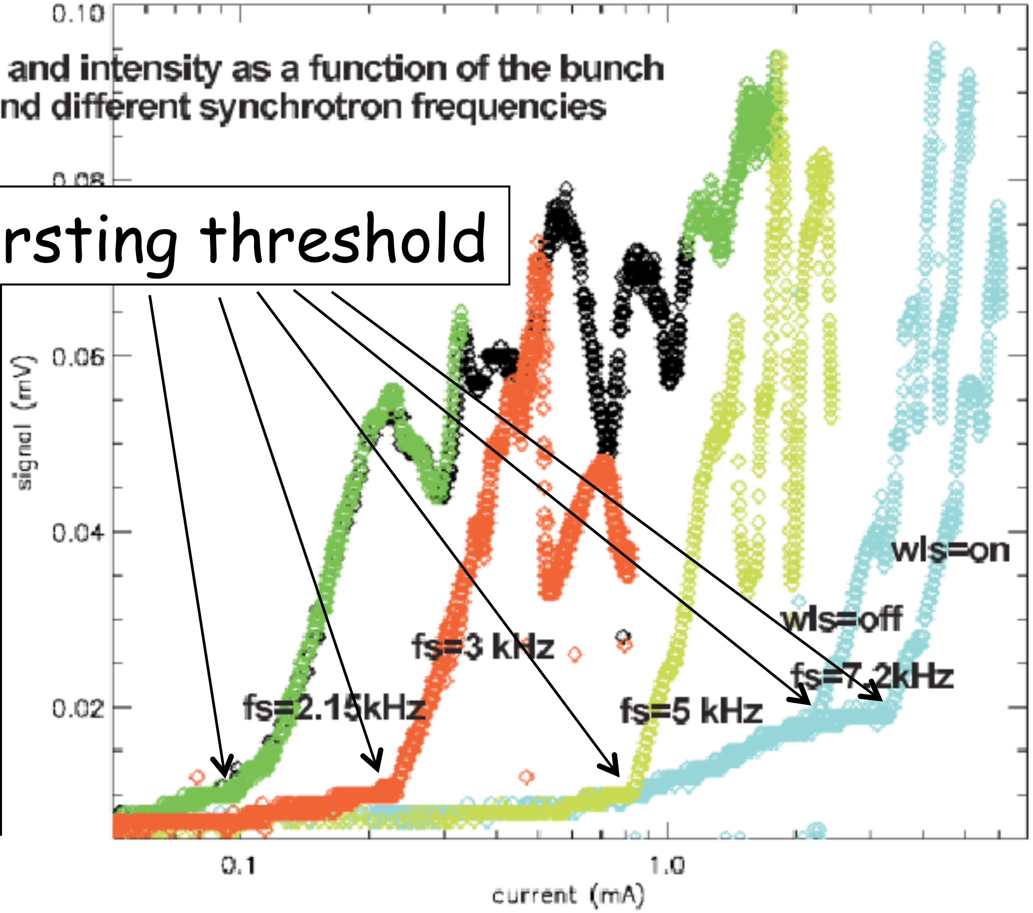

threshold and intensity as a function of the bunch current and different synchrotron frequencies

Bursting threshold

G. Wuestefeld, Napa CSR Workshop, Oct. 2002

Compare with theory

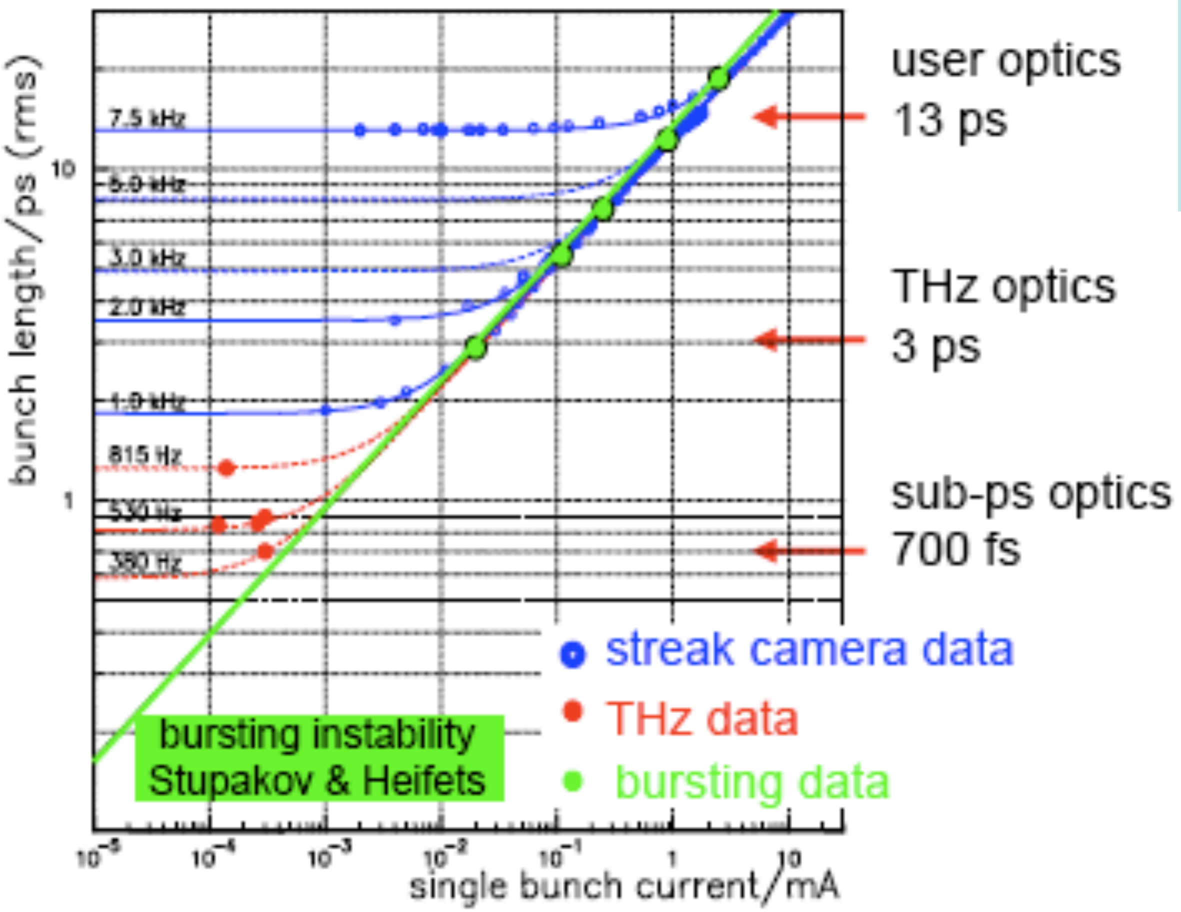

bunch length - current relation

user optics
13 ps

THz optics
3 ps

sub-ps optics
700 fs

CSR MBI (i.e. radiation impedance) could be responsible for most of the longitudinal single bunch effects in a storage ring.

Above threshold, peak current adjusts to stay at threshold.

$$\frac{\hat{I}\,|Z/n|}{2\pi\alpha\sigma_\delta^2(E/e)} \leq 1$$

Saturation model

Snapshot at time of saturation

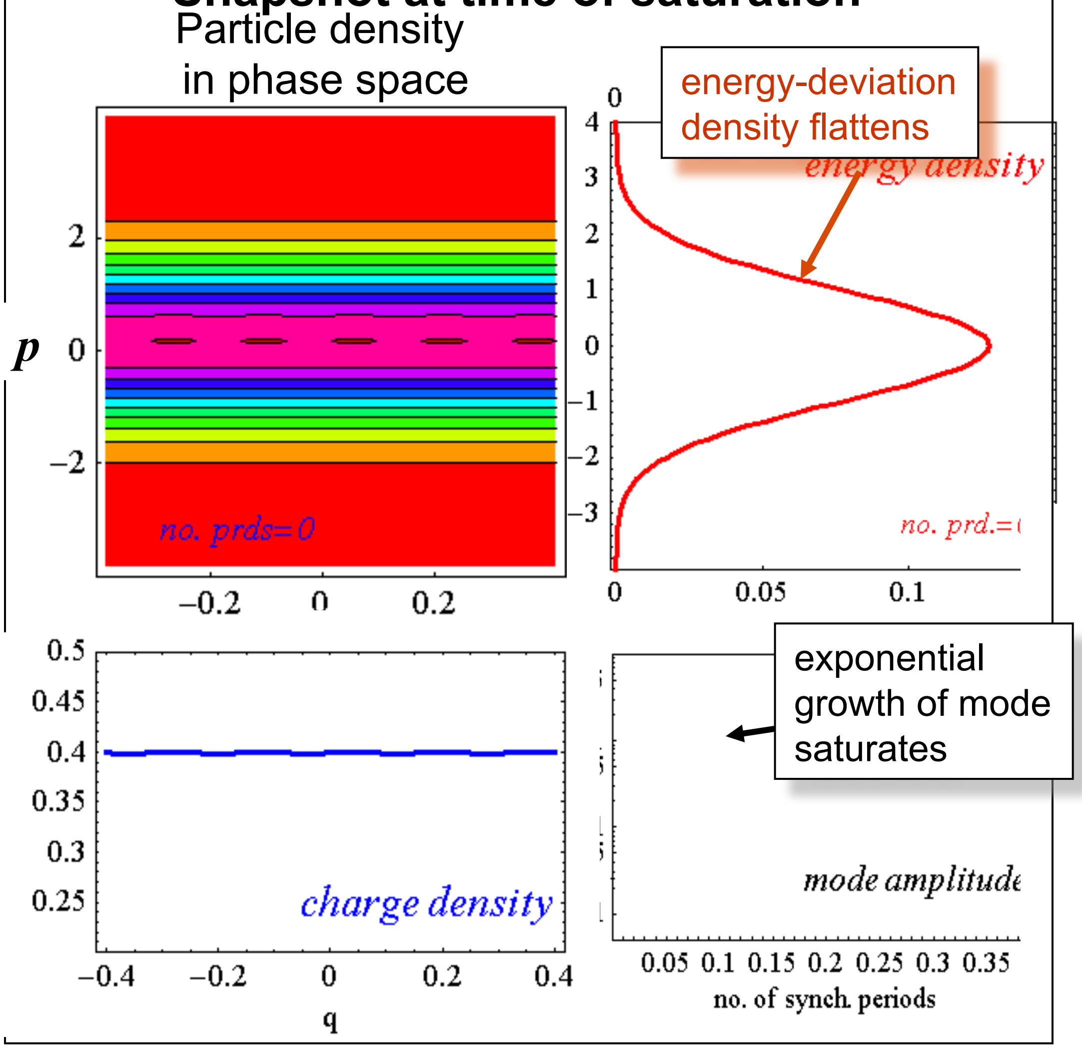

energy-deviation density flattens

exponential growth of mode saturates

ALS measurements (Jan 2005)

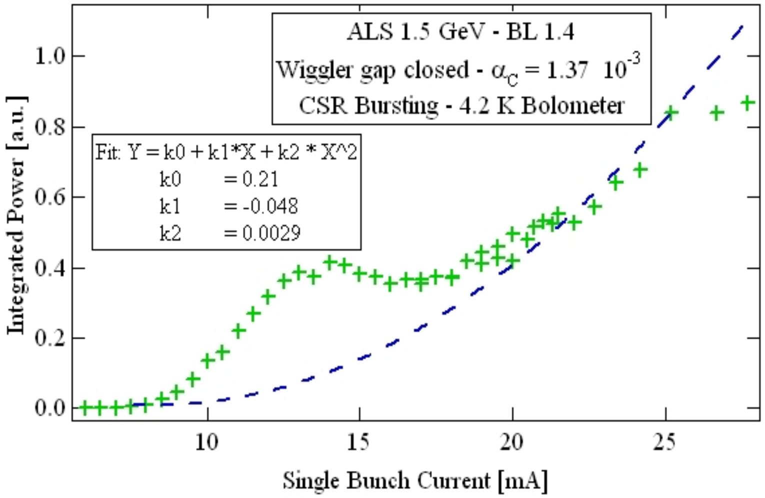

Simple model of saturation

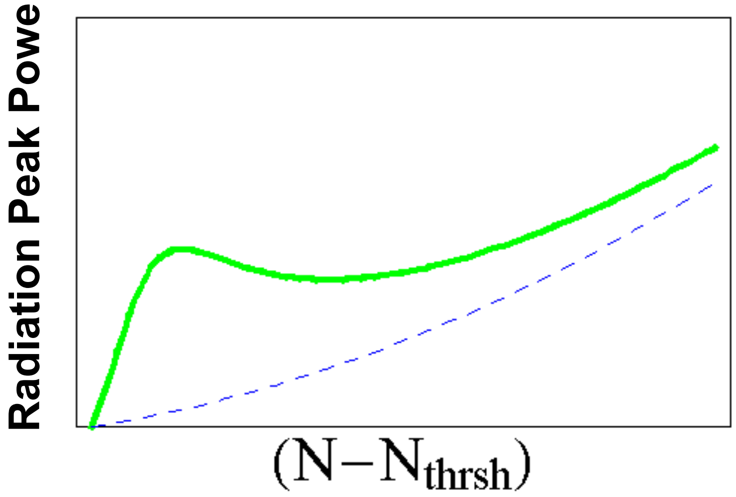

M. Venturini, et al. Phys. Rev. ST Accel. Beams 8, 014202 (2005)